0079-6611(94)00008-5

A dynamic optimization model of the diel vertical distribution of a pelagic planktivorous fish

RUNE ROSLAND[1] and JARL GISKE[1,2]

[1]*Department of Fisheries and Marine Biology, University of Bergen, Høyteknologisenteret,*
N-5020 Bergen, Norway
[2]*Institute of Marine Research, Postboks 1870 Nordnes, N-5024 Bergen, Norway*

Abstract – A stochastic dynamic optimization model for the diel depth distribution of juveniles and adults of the mesopelagic planktivore *Maurolicus muelleri* (Gmelin) is developed and used for a winter situation. Observations from Masfjorden, western Norway, reveal differences in vertical distribution, growth and mortality between juveniles and adults in January. Juveniles stay within the upper 100m with high feeding rates, while adults stay within the 100-150m zone with very low feeding rates during the diel cycle. The difference in depth profitability is assumed to be caused by age-dependent processes, and are calculated from a mechanistic model for visual feeding. The environment is described as a set of habitats represented by discrete depth intervals along the vertical axis, differing with respect to light intensity, food abundance, predation risk and temperature. The short time interval (24h) allows fitness to be linearly related to growth (feeding), assuming that growth increases the future reproductive output of the fish. Optimal depth position is calculated from balancing feeding opportunity against mortality risk, where the fitness reward gained by feeding is weighted against the danger of being killed by a predator. A basic run is established, and the model is validated by comparing predictions and observations. The sensitivity for different parameter values is also tested. The modelled vertical distributions and feeding patterns of juvenile and adult fish correspond well with the observations, and the assumption of age differences in mortality-feeding trade-offs seems adequate to explain the different depth profitability of the two age groups. The results indicate a preference for crepuscular feeding activity of the juveniles, and the vertical distribution of zooplankton seems to be the most important environmental factor regulating the adult depth position during the winter months in Masfjorden.

CONTENTS

1. INTRODUCTION

While early theories of vertical distributions focused on single factors such as light (BODEN and KAMPA, 1967; BLAXTER, 1976), food (HUNTLEY and BROOKS, 1982; GEORGE, 1983; GELLER, 1986), temperature (MCLAREN, 1963) or predation risk (IWASA, 1982), current models include the trade-off between several selective agents, e.g. food vs predation (MILINSKI and HELLER, 1978; GILLIAM and FRASER, 1987; JOHNSEN and JAKOBSEN, 1987; CLARK and LEVY, 1988; HOLBROOK and SCHMITT, 1988) or food vs predation vs temperature (LEVY, 1990). Trade-offs invoked have also been shown to depend on age (HOLTBY and HEALEY, 1990; WERNER, GILLIAM, HALL and MITTELBACH , 1983; WERNER and HALL, 1988), season (METCALFE and FURNESS, 1984; GISKE and AKSNES, 1992) and physiological condition of the animal (MILINSKI, 1985; JAKOBSEN, JOHNSEN and LARSSON 1988).

Using life history theory the input of several selective agents may be considered in a general expression yielding optimal solution for a habitat distribution (GILLIAM, 1982; WERNER and GILLIAM, 1984; AKSNES and GISKE, 1990; LEONARDSON, 1991; GISKE, AKSNES and FØRLAND, 1993). However, as this method works over generation times, it will not be able to resolve

differences in motivation over short time scales such as seasonal and diel cycles. Neither are such life history models capable of accounting for the physiological aspect, which is a strong motivational force in animal behaviour (COLGAN, 1993), and the method is therefore called 'static optimization'.

Over the last decade 'dynamic' optimization techniques [dynamic programming (CLARK and LEVY, 1988; HOUSTON, CLARK, MCNAMARA and MANGEL, 1988; YDENBERG, 1989; CLARK and YDENBERG, 1990a,b; SARGENT, 1990; BURROWS and HUGHES, 1991; BOUSKILA and BLUMSTEIN, 1992; MCNAMARA and HOUSTON, 1992; KELLY and KENNEDY, 1993), genetic algorithms (SUMIDA, HOUSTON, MCNAMARA and HAMILTON, 1990), Z-score models (STEPHENS, 1981) and optimal control theory (KATZ, 1974; SCHAFFER, 1983)] have therefore been applied in order to predict short-time and state dependent optimal behaviour. The ecological applicability of SDP is briefly described by MANGEL and CLARK (1986) and HOUSTON, CLARK, MCNAMARA and MANGEL (1988), and has been presented in a more detailed way by MANGEL and CLARK (1988).

We will study here the diel vertical distribution of two age groups of *Maurolicus muelleri* (Gmelin) during a winter day in Masfjorden (a fjord in western Norway). This is the same situation as studied by GISKE and AKSNES (1992), but here we will apply stochastic dynamic programming (SDP) instead of static life history models. The purpose of this work has been to validate the predictive power and robustness of a fairly simple model, based on SDP, by comparing the model predictions against observations from Masfjorden, and to elucidate some of the factors and mechanisms that underlie the observed vertical distribution of the fish.

M. muelleri is one of the numerically dominant mesopelagic fish species in most of the western fjords and off the continental shelf of Norway (GJØSÆTER, 1986). It is a planktivorous fish with a diet consisting of copepods and euphausiids (SAMYSHEV and SCHETINKIN, 1971; GJØSÆTER, 1981; YOUNG and BLABER, 1986). It has a maximum life span of 4 years and reaches maturity after one year at lengths about 40mm (GJØSÆTER, 1981). It breeds (in Norwegian fjords) between March and September (LOPEZ, 1979; GJØSÆTER, 1981) with an estimated maximum in May (LOPEZ, 1979).

Observations from Masfjorden in January (Fig.1) clearly indicate a difference in diel vertical distribution and feeding patterns among juveniles and adults (GISKE, AKSNES, BALIÑO, KAARTVEDT, LIE, NORDEIDE, SALVANES, WAKILI and AADNESEN, 1990; GISKE and AKSNES, 1992; BALIÑO and AKSNES, 1993). Juveniles stay within the upper 100m and have a distinct migration pattern throughout the diel cycle with surface encounters at dawn and dusk. They clearly respond (by altering vertical position) to instantaneous changes in the surface light during the day. Adults stay at depths between 100-150m and show no distinct vertical migration pattern. However, they do tend to respond to light changes during dawn and dusk and short time fluctuations in light intensity during the day. Stomach analyses of juveniles indicated high feeding rates (GISKE and AKSNES, 1992) and these obvservations correspond to data from YOUNG and BLABER (1986) who recorded high feeding activity for fish with body length <40mm in the periods preceding the breeding season. Stomach analyses of adults indicated very low feeding activity (GISKE, AKSNES, BALIÑO, KAARTVEDT, LIE, NORDEIDE, SALVANES, WAKILI and AADNESEN, 1990) resulting in a negative growth rate (GISKE and AKSNES, 1992).

The negative growth rates reported for adults in winter (GISKE and AKSNES, 1992) are incompatible with static optimization and resemble more the strategy of maximizing survival probability in a non-breeding period (cf STEPHENS, 1981, MCNAMARA, 1990). This is a problem which is readily simulated by SDP.

The model uses fitness as the optimization criterion, where fitness is given as a function of growth and survival, and positive growth is assumed to increase future reproductive output.
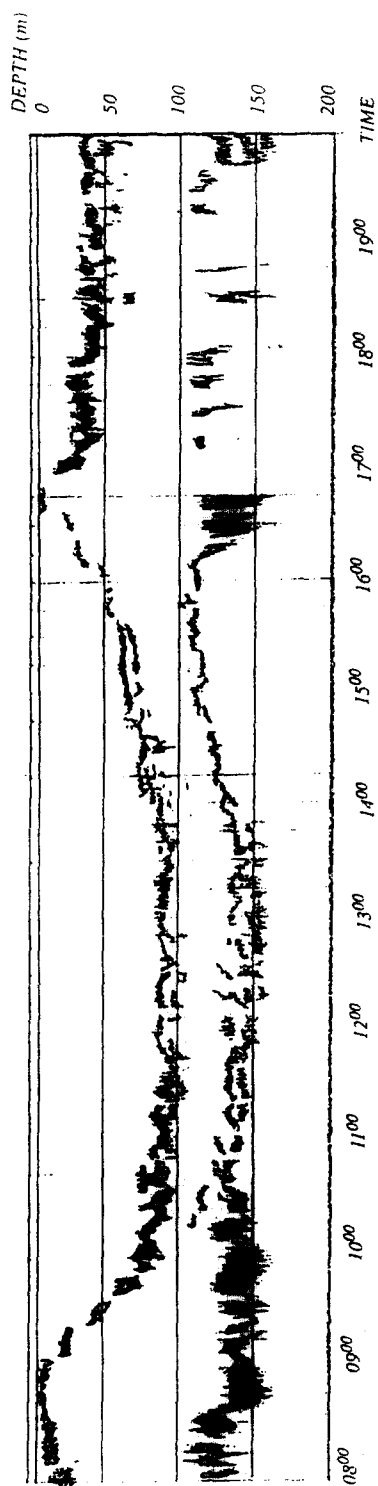
FIG. 1. Observed diel vertical distribution of *M. muelleri* in Masfjorden in January, redrawn from 120kHz echo diagrams. The upper layer is juvenile fish while the lower layer is adults.

AKSNES and GISKE (1990) suggested that there are two categories of animals, time manipulators and clutch manipulators, for which they derived different optimal life-history strategies. They concluded that time manipulators may benefit most by fast growth and high mortality, as the fitness reward by shortening the generation time balances the increased costs from predation. Clutch manipulators with fixed generation time will benefit most by reducing predation risk to maximize survival. Juvenile *M. muelleri* fit into the category of time manipulators as generation time can be defined as the time taken to reach maturity, whereas adults, for which spawning patterns are constant, fit into the category of clutch manipulators. Thus we assume that the observed differences in depth distributions in juvenile and adult *M. muelleri* in Masfjorden (GISKE, AKSNES, BALIÑO, KAARTVEDT, LIE, NORDEIDE, SALVANES, WAKILI and AADNESEN, 1990; BALIÑO and AKSNES, 1993) result from different feeding-mortality trade-offs between the two age groups.

2. MODEL

SDP provides an opportunity to calculate the sequential decisions (depth choice in this model) an animal makes over several time intervals, using fitness as the optimization criterion. Fitness is commonly expressed as a function of survival and fecundity; fecundity generally depends on age, size and physiological condition, whereas survival depends on both physiological state and predation risk. In non-breeding periods, optimal behaviour may therefore be regarded as the ideal balance between actions enhancing the physiological state (e.g. eating) and actions reducing mortality risk (e.g. hiding from predators) in order to maximize the future reproductive output. Animals at different physiological states face different needs, and are therefore expected to give different priority to different actions (e.g. predator avoidance and foraging).

The ultimate basis for this model is the relationship between fitness, growth and survival. *M. muelleri* is assumed to forage only by vision, and prey encounter rate is therefore given as a function of visual range, swimming speed and prey density. Growth rate depends on prey encounter rate, digestion rate, metabolic rate and indirectly on water temperature as metabolic processes are temperature regulated. Possible effects on feeding rate which results from competition between individuals, are not accounted for.

Observations on *M. muelleri* (KAWAGUCHI and MAUCHLINE, 1982; GISKE, AKSNES, BALIÑO, KAARTVEDT, LIE, NORDEIDE, SALVANES, WAKILI and AADNESEN, 1990; GISKE and AKSNES, 1992) and other mesopelagic fishes (KAWAGUCHI and MAUCHLINE, 1987; MAUCHLINE, 1991) indicate reduced growth during the winter months, probably as a result of low food abundance (KAWAGUCHI and MAUCHLINE, 1982). Mesopelagic fish also seem to allocate energy to fats and reproductive tissue rather than to size growth after maturity is reached (CHILDRESS, TAYLOR, CAILLIET and PRICE, 1980). Histological analyses of *M. muelleri* (FALK-PETERSEN, FALK-PETERSEN and SARGENT, 1986) support this view, as large fat deposits with a fat composition typical for energy reserves were found. Thus we assume that *M. muelleri* is capable of surviving periods with negative growth, and therefore we have excluded the possibility of starvation.

The habitats are represented as discrete depth cells along the vertical axis. As light decreases with depth and changes during the day, the habitats gradually change throughout the depth and time axis, and they are further differentiated by the various temperatures, prey sizes and prey densities along the vertical axis.

The main predators of *M. muelleri* in Masfjorden are the pelagic gadoids, blue whiting *Micrometistius poutassou* and saithe *Pollachius virens*. GISKE, AKSNES, BALIÑO, KAARTVEDT, LIE, NORDEIDE, SALVANES, WAKILI and AADNESEN (1990) found these fishes at all depths in

Masfjorden, with highest densities at 150-300m. Stomach samples combined with abundance estimates of the two year classes indicated that predation rates were 7 times higher for the juveniles than for the adults, in spite of the vertical profile of predators. When considering that the piscivores are able to relocate as easily as *M. muelleri*, representing predation risk by a profile of predator density will not be suitable in an optimization model. Rather, we make no specific assumption about the vertical distribution of the piscivores and relate predation risk to the visual range of the piscivores (cf GISKE, AKSNES and FIKSEN, 1994).

2.1 Terminal fitness function

M. muelleri has a long breeding period that starts in the late winter (early spring) and lasts to the end of the summer (LOPEZ, 1979; GJØSÆTER, 1981; YOUNG, BLABER and ROSE, 1987; ROBERTSON, 1976), and the adult fish produce several clutches during the breeding season (CLARK, 1982; MELO and ARMSTRONG, 1991). GJØSÆTER (1981) estimated maturity size about 40mm in Norwegian populations, but he found no significant correlation between fish size and egg number (egg numbers ranged between 200-500 with an average around 300).

We assume that increased growth increases the potential fecundity both for juveniles and adults, and that fish have to reach a minimum weight (about 0.6g at 40mm) to become mature. If this threshold weight is not attained until late in the breeding season, then fewer clutches may be produced, and if they do not reach maturity weight within the breeding season they have to delay reproduction until the following year (i.e. doubling of the generation time).

The time perspective of the model is a diel (24h) cycle in January and this raised a problem in generating a terminal fitness function based òn reproductive output. Therefore a tuned fitness function (Eq.1) was created, intuitively linked to the ontogenetic strategies suggested by GISKE and AKSNES (1992). We assume that starvation does not occur and that the relationship between fitness and growth remains constant during the 24h interval of this model, and so use a linear fitness function reflecting the long-term fitness reward of growth. The function is:

$$\Phi(W) = 1 + 100\gamma \left(\frac{W-W_0}{W_0} \right) \tag{1}$$

where W is fish weight at the terminal time, W_0 is initial weight and γ is the tuned constant determining the rate of increase of the function (given the value 0.007 and 0.002 for juveniles and adults, respectively). The constant γ was tuned to get the mortality in the basic run to be within the estimates from GJØSÆTER (1981) and GISKE, AKSNES, BALIÑO, KAARTVEDT, LIE, NORDEIDE, SALVANES, WAKILI and AADNESEN (1990). All fish of each age group are initiated at the same weight, 0.02 and 0.14g AFDW (0.1 and 0.7g wet weight) for juveniles and adults, respectively. The fitness function is shown in Fig.2.

2.2 Environmental parameters

2.2.1. Light and temperature. Surface light is calculated using a model for sun heights (SKARTVEIT and OLSETH, 1988). The sun declination Λ is given by:

$$\sin(\Lambda) = 0.3979\sin\{0.9856(D-80) + 1.9171[\sin(0.9856D) - 0.98112]\} \tag{2a}$$

where D represents the day of the year (ranging from 0-365). The horizontal angle ($\varnothing$) between
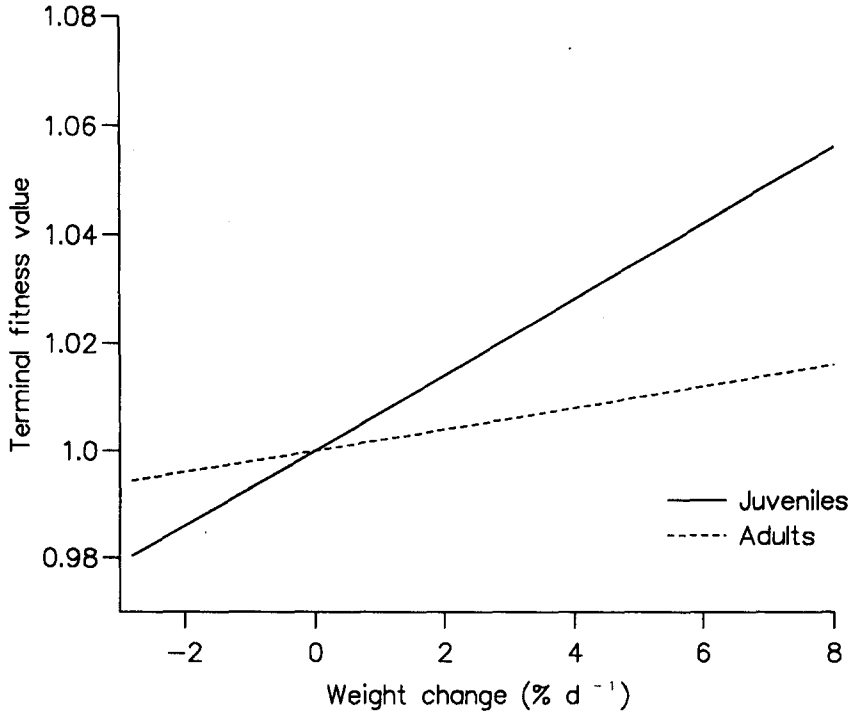
FIG.2. Terminal fitness reward for juvenile and adult fish at different growth rates. Growth is given as weight change (% of initial body weight) obtained during the 24h cycle. The rate of increase of the function is set to 0.007 and 0.002 for juvenile and adult fish, respectively.

the sun position and north at each hour of the day is given by:

$$\emptyset = 15H \tag{2b}$$

where H is the hour of the day. Sinus (h_d) of the sun height is:

$$h_d = \sin(\Lambda) \sin(B) - \cos(\Lambda) \cos(B) \cos(\emptyset) \tag{2c}$$

where B is the latitude. Maximal light intensity (I_{max}) observed at Masfjorden (GISKE, AKSNES, BALIÑO, KAARTVEDT, LIE, NORDEIDE, SALVANES, WAKILI and AADNESEN, 1990) is used to calculate a solar constant (I_0). This value was found using the sinus value of the sun height at midday (maximum sun height):

$$I_0 = \frac{I_{max}}{h_d} \tag{3a}$$

and used to calculate surface light I_s during the day at different sun heights:

$$I_s(H) = I_0 h_d \tag{3b}$$

The surface light (μmol $m^{-2}s^{-1}$) during the diel cycle is given in Fig.7. (Maximal surface light occurs at 1200h from Eqs 2-3, but the time axis of the model is adjusted in order to get surface light maximum at the same time as in western Norway in winter, at 1230h.) The surface light intensities at night, when the sun is below the horizon, and it is calculated by extrapolations between light intensities given by ROSENBERG (1966) at sun heights at 6, 12 and 18° below the horizon. Light intensity is assumed equal for all sun heights more than 18° below the horizon (ROSENBERG, 1966). (The deviation from a sinusoidal shape of the surface light between dusk and dawn in Fig.7 results from this extrapolation between light intensities at night.)

The depth integrated diffuse light attenuation coefficient (k) is given in Fig.3a, and it is based on data from GISKE, AKSNES, BALIÑO, KAARTVEDT, LIE, NORDEIDE, SALVANES, WAKILI and AADNESEN (1990). The observational data only covered the depths from surface to 70m, but as the local diffuse attenuation coefficient each depth seemed to stabilize at $0.08m^{-1}$ below 16m, the depth integrated diffuse attenuation coefficient could be recalculated for 16-250m using this value ($0.08m^{-1}$). The recalculated value of k gave an almost exact match with the observed k down to 70m. The local beam attenuation coefficient (c) is assumed to be 3 times higher than the local diffuse attenuation coefficient (KIRK, 1981).

The depth profile of the temperature is given in Fig.3b, where temperature ranges between 5°C at surface and 9.7°C at 45m (GISKE, AKSNES, BALIÑO, KAARTVEDT, LIE, NORDEIDE, SALVANES, WAKILI and AADNESEN, 1990).

2.2.2. Zooplankton. During winter most zooplankton groups in Masfjorden seem to have a static depth distribution (GISKE, AKSNES, BALIÑO, KAARTVEDT, LIE, NORDEIDE, SALVANES, WAKILI and AADNESEN, 1990). The zooplankton was sampled with Juday net and MOCNESS trawl at 50m depth intervals from surface to bottom (GISKE, AKSNES, BALIÑO, KAARTVEDT, LIE, NORDEIDE, SALVANES, WAKILI and AADNESEN, 1990), and the zooplankton depth profile used in the model was created by linear interpolations between the centre of the sampling intervals (0-50m, 50-100m, 100-150m, 150-200m, 200-250m). The depth profile of zooplankton abundance (ind. m^{-3}) and mass (μg AFDW $ind.^{-1}$) is given in Fig.4.

2.3 Processes

2.3.1. Vision. The ability to detect food is assumed to depend on the visual range which is a function of surface light, water clarity, size and contrast of the prey and the capability of the fish to sense differences in light intensity (AKSNES and GISKE, 1993):

$$r^2 = \rho(I_s \exp(-cr-Kz)) \, | \, C_0 \, | \, \pi l^2 \Delta S_e^{-1} \tag{4}$$

where r is visual range, ρ is fraction of light passing the air-sea interface, I_s is irradiance in the air at the sea surface, K is depth integrated diffuse attenuation coefficient, z is depth, C_0 is inherent contrast of the visual object, c is beam attenuation coefficient, l is prey radius, and ΔS_e is the sensitivity threshold of the eye. The equation is solved by a Newton-Raphson iteration method (ROSLAND, 1993).

The sensitivity threshold of the eye (ΔS_e) is not known, but has been adjusted in order to get the adult encounter rate at the observed depths to be within the ranges observed in Masfjorden; about 5 copepods per day (GISKE, AKSNES, BALIÑO, KAARTVEDT, LIE, NORDEIDE, SALVANES, WAKILI and AADNESEN, 1990, GISKE and AKSNES, 1992). Based on measurements of lens
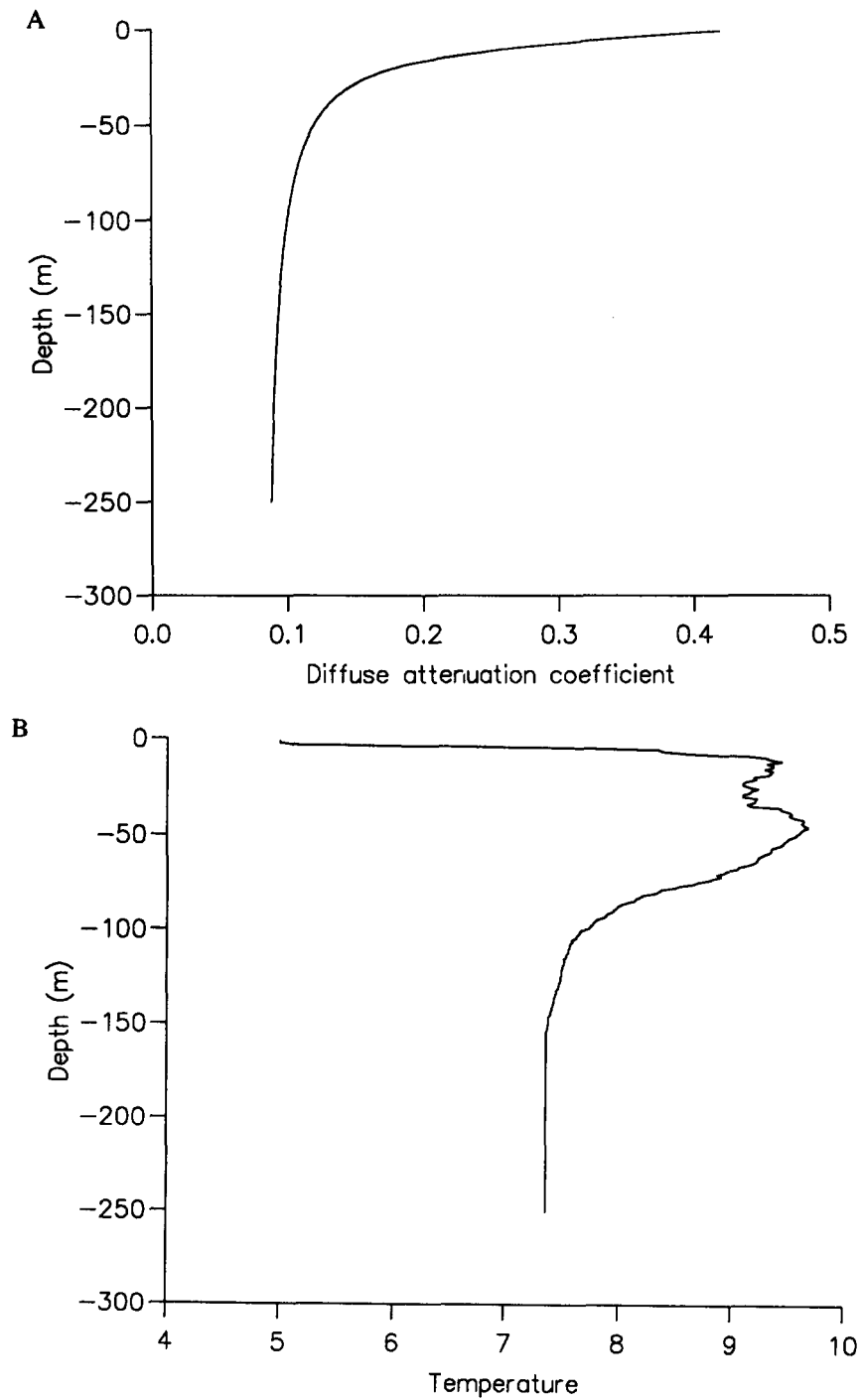
FIG.3. (A) Vertical profile of depth integrated diffuse light attenuation coefficient (m^{-1})
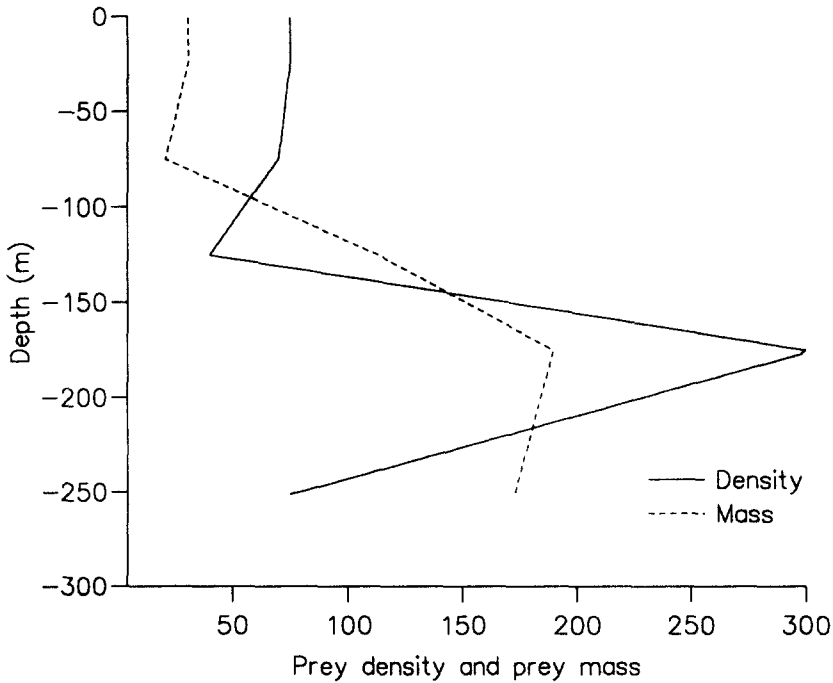(B) Vertical profile of temperature (°C).

FIG.4. Vertical distribution of zooplankton abundance (ind. m^{-3}) and mass (μg AFDW ind.$^{-1}$;).

diameters, the juvenile visual threshold was estimated to be 4 times higher than the adult visual threshold (GISKE and AKSNES, 1992).

The zooplankton radius is calculated from mass, assuming a cubic shape and a weight volume relation of 1cm^3 = 1g wet weight (GISKE and AKSNES, 1992):

$$l = \left(\frac{3}{4\pi} w_w \right)^{1/3} \tag{5}$$

where w_w is prey wet weight. The radius of *M. muelleri* was set at half the fish length.

2.3.2. Encounter rate. The prey encounter rate depends on prey density and the volume of water that passes the visual field of the animal. The visual field area (A) is a function of visual range and visual field angle (θ):

$$A = \pi(r\sin\theta)^2 \tag{6a}$$

The visual prey encounter rate (E) can then be expressed by visual area, swimming speed (v) and prey density (N):

$$E = AvN \tag{6b}$$

Average cruising speed of the fish was set to be one fish length per second (PRIEDE, 1985; CLARK and LEVY, 1988). This expression represents the maximum visual prey encounter rate and

does not account for prey handling time. Including handling time, h, gives an expected maximal handling limited prey ingestion rate (e) (AKSNES and GISKE, 1993):

$$e = \frac{h^{-1}N}{(Avh)^{-1} + N} \tag{6c}$$

This equation is analogous to the Michaelis-Menten equation, where the 'half saturation' coefficient is expressed by $(Avh)^{-1}$. Prey encounter is further assumed to be Poisson distributed with expectation equal to the handling limited prey ingestion rate (e, Eq.6c) multiplied by time. The probability of m (ind) prey encounters at depth z during a time interval of length τ is then:

$$P_z(m) = \frac{(e\tau)^m}{\exp(e\tau)m!} \tag{7a}$$

Feeding rate may be limited by either visual encounter rate, handling time, or by the stomach capacity (Δs). As Eq.6c includes both handling time and visual encounter rate, feeding rate f (g, $g^{-1}s^{-1}$) can be defined as a minimum function of e (Eq.6c) and Δs:

$$f = \min[F_m, \Delta s/(W_0\tau)] \tag{8a}$$

where

$$F_m = (e\, w_p)/W_0 \tag{8b}$$

and

$$i_c = \text{int}\{\Delta s/(W_0 t)\} \tag{8c}$$

and W_0 is initial body weight (AFDW).

The probability of maximum prey consumption (i_c) where stomach capacity is reached is found by:

$$P_z(i_c) = 1 - \sum_{m=0}^{(i_c - 1)} P_z(m) \tag{7b}$$

2.3.3. Metabolism. The physiological system is represented by the stomach (s). Observations from Masfjorden (GISKE, AKSNES, BALIÑO, KAARTVEDT, LIE, NORDEIDE, SALVANES, WAKILI and AADNESEN, 1990) gave an estimate of stomach capacity of about 20 copepods for adults and 15 for juveniles. Using the average copepod size in the observed depth ranges of juveniles and adults gave a stomach load capacity of about 2% of body weight (AFDW) for both age groups. The state dynamics of the stomach are:

$$s_n = s + mw_p - \sigma \tag{9a}$$

where s and s_n are stomach contents at start and the end of the time interval, respectively, m is prey

items eaten during the time interval, w_p is prey mass (AFDW) and σ is stomach contents evacuated during the time interval. Stomach evacuation is described by an exponential function (JOBLING, 1981):

$$\sigma = s(1-\exp(-\kappa\tau)) \tag{9b}$$

where k is evacuation rate (see Eq.12a for temperature effects on κ).

In order to calculate growth, a dynamic state variable tracing the mass (growth) budget during the modelling period was defined (w). The dynamics of this variable (assimilated mass) is a function of mass evacuated from the stomach minus the metabolic costs (i.e. a fish that does not eat will have a net weight loss). The dynamics of this variable is given by:

$$w_n = w + \sigma\alpha - c_m - c_m \left[\frac{\varepsilon \, | \, d-z \, |}{\tau} \right] \tag{10a}$$

Here w_n and w is the state of the assimilation (growth) variable at the end and start of the time interval, respectively, α is assimilation coefficient, c_m is metabolic cost in time interval, d is depth position entering the time interval, z is depth position during the time interval and ε represents the energetic costs by migrating from d to z. Vertical migration probably requires energy for pressure adjustments to the swim-bladder (ALEXANDER, 1972; SCHMIDT-NIELSEN, 1983) and also energy for swimming if rapid migration. We did not want to incorporate advanced submodels for energetics of vertical migration and therefore made an 'ad hoc' function, with a linear connection between energy consumption and vertical migration distance (ε). As both feeding rate and mortality rate are very low during night, the representation of temperature for metabolic processes will be deterministic for night time distribution. Thus, if vertical migration requires no energy, it should be profitable for adult fish to stay at the surface where it is cold during night thereby reducing the metabolic rate and saving energy. However, observations show that they do not apply this strategy indicating that the energetic requirements for migration to the surface at night is too high. The cost of vertical migration (ε) was therefore calibrated to a level where adult fish failed to move to the surface at night. (It should be noted that juveniles, for which surface migration leads to increased feeding rate, are much less sensitive to ε as the energetic benefits from feeding far exceed the energetic loss resulting from vertical migration.)

The metabolic costs c_m in each time interval is calculated from metabolic cost rate R (see Eq.12b for temperature effects on R):

$$c_m = W_0[1-\exp(-R\tau)] \tag{10b}$$

where W_0 is initial body weight.

   2.3.4. Migration constraints. Migration distances must be limited by swimming speed and the time needed for pressure adjustments of the swim-bladder, and so it was necessary to include the depth position of fish as a state variable and define a maximal vertical migration rate (δ, m s^{-1}) in order to get a realistic vertical migration pattern during the time intervals. Therefore optimal depth, z*(s,w,d,t), during time intervals is found from a limited depth range dependent on the depth position (d) at the start of the time interval:

$$d - (\delta\tau) \leq z^*(s,w,d,t) \leq d + (\delta\tau) \tag{11}$$

As for ε, the value of δ is not known, but was set to $2.78 \ 10^{-2} m \ s^{-1}$ based on the observed migration rates from Masfjorden (BALIÑO and AKSNES (1993).

2.3.5. Temperature effects. An exponential relationship between metabolic parameters and temperatures is assumed with a doubling of metabolic rates with a temperature increase of 10°C ($Q_{10} = 2$) (SCHMIDT-NIELSEN, 1983). If T represents temperature in degrees Celsius the relation between stomach evacuation rate and temperature is:

$$\kappa = \kappa_0 exp(0.0693T) \tag{12a}$$

where κ_0 is stomach evacuation rate at 0°C. The value of κ_0 was adjusted to get $\kappa \sim 1.9 \ 10^{-4} s^{-1}$ at maximum temperature, according to data from WINDELL (1978). The effect of temperature on daily rate of metabolic costs is similarly expressed:

$$R = R_0 exp(0.0693T) \tag{12b}$$

where R_0 is metabolic cost rate at 0°C. This value was adjusted to match data from KIØRBOE, MUNK and RICHARDSON (1987) for herring larvae (Table 1).

2.3.6. Mortality by predation. The mortality risk depends on the visual range (Eq.4) of the predator, and instantaneous mortality is expressed from predator visual range (depth dependent) and a tuned constant k_m:

$$M = r^2 k_m \tag{13a}$$

where M is the instantaneous mortality in each depth. The sensitivity threshold of the predator's eye (ΔS_e) is unknown, but the given value ($10^{-5} \mu mol \ m^{-2} s^{-1}$) results in a visual range of about 4-5m near the surface at midday. (Variations of the predators' sensitivity threshold had little effect on the vertical profile of predation risk.)

GJØSÆTER (1981) estimated an instantaneous mortality of $1.8 y^{-1}$ which gives a daily instantaneous mortality of $4.9 \ 10^{-3} d^{-1}$. However, with the low feeding activity observed in adults in January (GISKE and AKSNES, 1992), mortality is probably less than the yearly average. Rough estimates from Masfjorden (GISKE, AKSNES, BALIÑO, KAARTVEDT, LIE, NORDEIDE, SALVANES, WAKILI and AADNESEN, 1990) indicated juvenile mortality of $0.016 d^{-1}$ and adult mortality of $2.2 \ 10^{-3} d^{-1}$, and the mortality constant (k_m) was tuned to get daily adult mortality (M) in the observed depth ranges to be about 0.1%. Surviving probability φ_z at depth z during a time interval of length τ is then:

$$\varphi_z = exp(-M\tau) \tag{13b}$$

2.4 The dynamic equations

The dynamic equations have basically the same structure as given by MANGEL and CLARK (1988), and linear interpolation is used to find fitness for values of states falling between the discrete steps in the state variable arrays. We only give the equations of the forward iteration here, as the back iteration is in principle equal.

The conditional state change probability functions are given in Eqs 14a-b:

TABLE 1: Environmental and biological parameter with values used in the basic run. The indices J, A and P refer to juvenile, adult and predator, respectively. AFDW = ash free dry weight.

Symbol	Variable description	Unit	Value	Source
α	assimilation coefficient		0.7	(7)
δ	depth migration rate	m s^{-1}	2.78 10^{-2}	(2)
ε	migration cost coefficient	s m^{-1}	45	
γ	terminal fitness coefficient		0.07(J), 0.002(A)	
κ	stomach evacuation rate	s^{-1}		
κ_0	stomach evacuation rate at 0°C	s^{-1}	1 10^{-4}	(8)
Λ	sun declination	degrees		
θ	visual field angle	degrees	30	(4)
ρ	light passing the sea-air interface		0.5	(1)
σ	evacuation from stomach during a time interval	μgAFDW		
τ	duration of time interval	s	900	
A	visual area	m^2		
B	latitude	degrees	61	
c	local beam attenuation coefficient	m^{-1}	0.24-1.26	(5)
c_m	metabolic costs in time interval	μgAFDW		
C_0	inherent contrast of visual object		0.5	(1)
D	day of the year in Julian calendar		1-365	
d	depth position at start of a time interval	m	1-201	
E	visual prey encounter rate	ind. s^{-1}		
e	handling limited prey encounter rate	ind. s^{-1}		
F	terminal fitness function connected to state			
F_m	handling limited mass encounter rate	g g^{-1}s^{-1}		
f	feeding rate	g g^{-1}s^{-1}		
H	hour of day		1-24	
h_d	sinus of sun height above horizon	degrees		
h	prey handling time	s ind.$^{-1}$	2	(3)
I_0	recalculated surface light maximum constant	μmol m^{-2}s^{-1}		
I_{max}	observed surface light maximum	μmol m^{-2}s^{-1}	70	(5)
I_s	surface light at different times of day	μmol m^{-2}d^{-1}		
i_c	maximal prey items ingested (stomach limited)	ind.		
K	depth integrated diffuse attenuation coefficient	m^{-1}	0.09-0.42	(5)
k_m	mortality constant	m^{-2}s^{-1}	2.55 10^{-6}	
l	radius of prey (zooplankton)	m	4 10^{-4} - 8.6 10^{-4}	
M	instantaneous mortality rate	s^{-1}		(6), (5)
m	prey items encountered in a time interval	ind.		
	maximal prey ingested (stomach limited)	ind.		
N	prey density	ind. m^{-3}	40-300	(5)
R	metabolic cost rate	s^{-1}		
R_0	metabolic cost rate at 0°C	s^{-1}	1.7 10^{-7}	(7)
r	visual range	m		
ΔS_e	sensitivity threshold of eye	μmol m^{-2}s^{-1}	3 10^{-6}(J), 7.5 10^{-7}(A), 1 10^{-5}(P)	
Δs	free space of stomach	μgAFDW	0-440(J)	(5)
T	temperature	°C	5-9.47	(5)
v	fish swimming speed	m s^{-1}	0.021(J), 0.047(A)	
W	terminal (final) fish weight	μgAFDW		
W_0	initial fish weight	μgAFDW	2200(J), 144000(A)	(5)
w_p	dry weight of prey	μgAFDW ind.$^{-1}$	21-190	(5)
w_w	wet weight of prey	kg wet weight	(AFDW*14)	(5)
$\emptyset$	horizontal angle between sun's position and north	degrees	0-360	

References:
(1) AKSNES and GISKE (1993); (2) BALIÑO and AKSNES (1993); (3) EGGERS (1976); (4) GISKE and AKSNES (1992);
(5) GISKE, AKSNES, BALIÑO, KAARTVEDT, LIE, NORDEIDE, SALVANES, WAKILI and AADNESEN (1990);
(6) GJØSÆTER (1981); (7) KIØRBO, MUNK and RICHARDSON (1987); (8) WINDELL (1978).

$$A_m(s_n,w_n,z,t+1 \mid s,w,d,t) = \varphi_z \cdot P_z(m) \tag{14a}$$

$$S_m(s_n,w_n,z,t+1 \mid s,w,d,t) = (1-\varphi_z) \cdot P_z(m) \tag{14b}$$

where A_m and S_m are the conditional probabilities that the new states s_n, w_n, z at time t+1 are reached, given that the former states are s, w, d at time t. The subscript m denotes prey items ingested (0-i_c). A_m is the probability that the fish survives and S_m is probability that the fish is eaten, φ_z is survival probability and $P_z(m)$ is probability of m prey ingested at depth z. The state distribution of fish alive is then:

$$\eta(s_n,w_n,z,t+1) = \sum_{s,w,d,m} A_m (s_n,w_n,z,t+1 \mid s,w,d,t) \cdot \eta(s,w,d,t) \tag{15a}$$

where $\eta(s_n,w_n,z,t+1)$ is fraction of population alive at time t+1 at state s_n,w_n. Fraction Z(t) dying as a result of predation during time interval t is:

$$Z(t) = \sum_{s,w,d,m} S_m(s_n,w_n,z,t+1 \mid s,w,d,t) \cdot \eta(s,w,d,t) \tag{15b}$$

The depth distributions of the population throughout all time intervals (t=1,2...T-1,T) are calculated by defining a depth fraction variable U(z,t) that counts fractions of fish alive at each depth:

$$U(z,t) = \sum_{s,w,d} \eta(s,w,d,t) \mid z^*(s,w,d,t) = z \tag{16}$$

TABLE 2: Variables in the dynamic equations. (AFDW = ash free dry weight.)

Symbol	Variable description	Unit	Value
φ_z	survival probability at depth z		
η	fraction of fish surviving time interval		
A_m	probability of surviving time interval		
d	depth position of fish at start of a time interval	m	1-201
F	terminal fitness function connected to state		
S_m	probability of being eaten in time interval		
P_z	probability of m encounters (Poisson) at depth z		0-1
s	stomach contents at beginning of a time interval	μgAFDW	
s_n	stomach contents at end of a time interval	μgAFDW	
U	variable for depth location in the time intervals		
w	assimilated weight at start of a time interval	μgAFDW	
w_n	assimilated weight at end of a time interval	μgAFDW	
Z	fraction of fish eaten in time interval		
z	depth position of fish at end of time interval	m	0-201
z^*	optimal depth choice during a time interval	m	0-201

2.5 Simulation protocol

A basic run was established with parameter values (Tables 1 and 2, Figs 2-3 and 7) based on data from Masfjorden (GISKE, AKSNES, BALIÑO, KAARTVEDT, LIE, NORDEIDE, SALVANES,

WAKILI and AADNESEN, 1990), and the model was then tested for sensitivity to different parameters (Table 3). The parameters were changed roughly within ranges of what occurs in the natural environment as we wanted to see which factors that may exercise the greatest influence on distribution, growth and survival. The model was also run with doubled time horizon (not included in Tables 3 and 4) as a stationarity test.

Many of the figures presented are based on averages of the two age groups (feeding rate, growth rate, etc.). These average values are calculated by multiplying fraction of fish choosing depth z (Eq.15a) with the parameter of interest (stomach fullness, feeding rate, etc.), thereby obtaining a weighted average of the parameter.

The modelled period covers a 24h cycle, but within the time interval from 1900-0700 surface light is at the minimum and the modelled vertical distribution, feeding rates and mortality are static. We therefore chose to give figure representations within the period of changes (0700-1900).

A documentation of the computer program (FORTRAN) and input data are given by ROSLAND (1993).

TABLE 3. Sensitivity analyses: factor of parameter change from basic run.

Run no.	Variable changed from the basic run	Changed by factor	Symbol
1	Prey density	0.5	N
2	-	2	-
3	Prey mass, radius	$0.3, 0.3^{1/3}$	W_p, l
4	-	$3, 3^{1/3}$	-
5	Mortality constant	0.5	k_m
6	-	2	-
7	Surface light	0.1	I_{max}
8	-	10	-
9	Temperature	0.7	T
10	-	1.4	-
11	Stomach evacuation rate	0.5	κ_0
12	-	2	-
13	Fitness function	0.25	g
14	-	4	-

3. RESULTS

3.1 The basic run

The depth profile of the handling-limited prey ingestion rate (e, ind.h^{-1}) and predation risk (M,h^{-1}) at midday (1230h) are given for juveniles and adults in Fig.5a. The handling-limited prey ingestion rate decreases with depth and is affected by variations in zooplankton abundance and size (Fig.4). As a result of a lower sensitivity threshold of the eye and higher swimming speed adults have a higher potential ingestion rate than juveniles.

Predation risk generally shows fewer irregularities with depth since density dependent functions are not included in predation risk. Predation risk is also higher for adults since they are larger than juveniles, and therefore more visible to the predators.

Water turbidity increases quite strongly in the upper 20m, resulting in increased beam attenuation coefficients (c in Eq.4). This effect works counter to the positive influence from

increased light intensity and the effect is amplified with increased visual ranges. This is quite evident in the curve for predation risk (Fig.5a) which decreases above 20m. The increased water turbidity near the surface has less effect on the prey encounter rate of *M. muelleri* because its visual range is relatively short and therefore not affected by the reduced water transparancy to the same extent as its piscivorous predators (cf FIKSEN, 1993; GISKE, AKSNES and FIKSEN, 1994).

TABLE 4. Results from basic run and sensitivity analyses. Average light intensity of juveniles and adults at midday (1130-1330) and dusk (1600-1700). If maximum peaks in light intensity occur at dawn these peak values are listed, else the average value during the time interval is used. Average diel feeding rates, growth rates, mortality rates and depth position at daytime are given. In columns with % heading, the values represent the percentage deviation from basic run (i.e. $100 \cdot X_i/X_{basic}$). V and S indicate visual and stomach limited feeding rate during daytime, respectively.

|		Light intensity in layer		Feeding limitation	Feeding	Mortality	Growth	Depth
		Midday	Dusk					
Basic run		$(mmol\ m^{-2}s^{-1})$			$(g\ g^{-1}d^{-1})$	(d^{-1})	$(g\ g^{-1}d^{-1})$	(m)
Juveniles		844E-02	.287E-01	V	.099	.02100	.0428	86
Adults		.541E-04	.631E-06	V	.004	.00018	-.0211	141
Sensitivity analyses	%	%	%		%	%	$(g\ g^{-1}d^{-1})$	(m)
Juveniles								
Prey density	50	35.0	1397.2	V	63	77	.0186	91
-	200	116.1	55.7	V	115	68	0.529	79
Prey size	30	15.6	2700.3	V	42	79	.0035	101
-	300	39.8	33.1	S	121	33	.0570	90
Mortality constant	50	395.7	111.1	S	116	76	.0543	61
-	200	35.0	159.2	V	68	99	.0220	91
Surface light	10	234.6	79.1	S	111	111	.0511	40
-	1000	89.2	104.2	S	102	66	.0443	110
Temperature	70	83.2	114.6	V	86	82	.0369	87
-	140	282.0	121.3	V	129	141	.0567	70
Stomach evacuation	50	35.2	65.5	V	59	49	.0154	91
-	200	372.0	145.3	V	169	175	.0864	67
Fitness function	25	15.4	0.1	V	12	4	-.0150	102
-	400	395.7	134.5	S	118	162	.0556	61
Adults								
Prey density	50	44.9	44.8	V	38	45	-.0230	151
-	200	100.0	100.0	V	200	100	-.0180	141
Prey size	30	9.1	9.0	V	5	9	-.0240	171
-	300	857.7	10^6	S	2062	3090	.0376	118
Mortality constant	50	1200.0	100.0	V	100	50	-.0211	141
-	200	44.9	44.8	V	76	90	-.0218	151
Surface light	10	4.7	44.8	V	12	7	-.0238	151
-	1000	977.8	100.0	V	916	903	.0043	141
Temperature	70	100.0	100.0	V	100	100	-.0176	141
-	140	100.0	706.8	V	101	130	-.0258	141
Stomach evacuation	50	100.0	100.0	V	100	100	-.0211	141
-	200	100.0	100.0	V	100	100	.0211	141
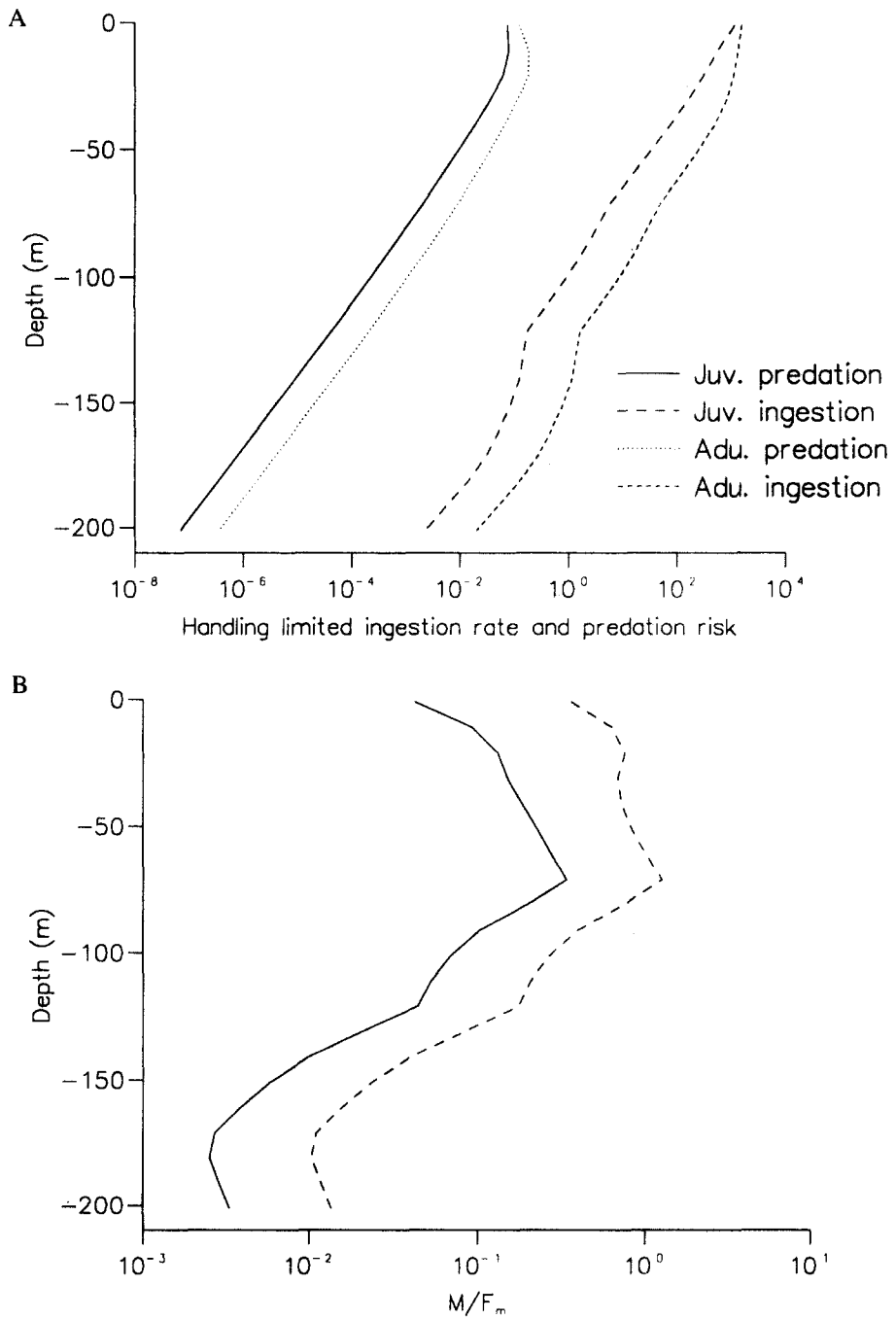
FIG.5. (A) Predation risk (M, h^{-1}) and handling limited ingestion rate (e, ind. h^{-1}) for juveniles and adults at midday. (B) Depth variations in the predation risk (M, h^{-1}) on handling limited ingestion rate (F$_m$, g g^{-1}h^{-1}), 'M/F$_m$ ratio', for juvenile (solid) and adult (dotted) fish.
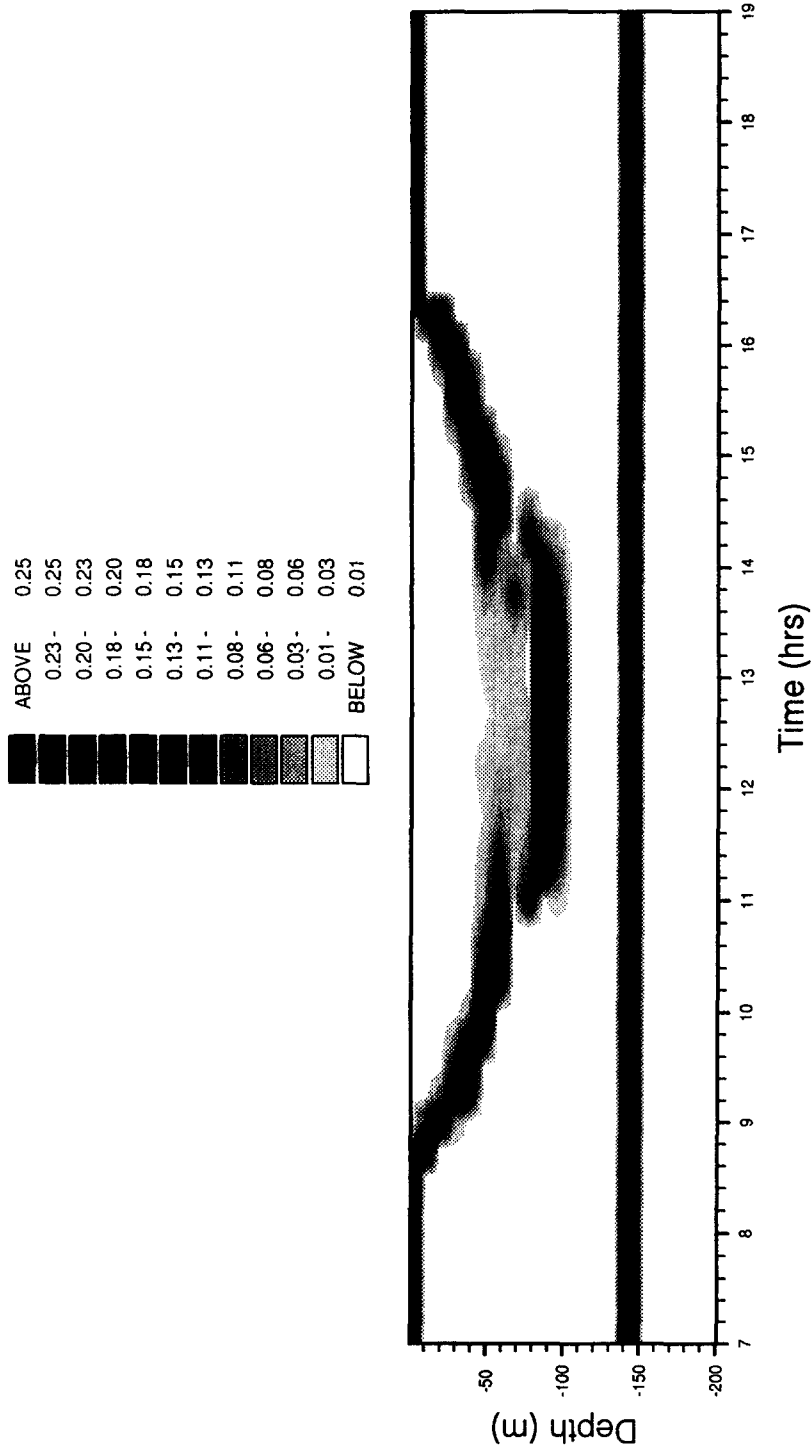
FIG.6. Diel vertical distribution of juveniles (upper layer) and adults (lower layer) in the basic run. The scale at the top indicates the fraction of the population at each depth.

The vertical distribution of the juvenile layer (Fig.6) clearly correlates with surface light intensity (Fig.7). Juveniles leave the surface around 0845h and descend to about 60-90m at midday the layer splits into two strata, one at 91m (~86% of the layer) and the other at 81-61m (~14% of the layer). Towards dusk the juvenile layer starts ascending, reaching the surface around 1630h where it stays throughout the night (Fig.6). The light intensity in the juvenile layer varies during the day with intensities increasing at dawn and dusk (Fig.7, Table 4). Feeding rate and mortality rate vary according to the light intensity of the layer (Fig.8a,b) with maximum values in the crepuscular periods. The feeding maximum at dawn is about 7 times the daytime level as a result of stomachs being empty after a long night without feeding. During the night both feeding rates and mortality are undetectably low.

During the day in the shallow waters the light intensity becomes high enough for prey encounter rate to exceed the evacuation rate of the stomach, and feeding becomes limited by digestive processes. As surface light varies during day, the depth at which the limitation on feeding rate shifts from digestion to prey encounter, will also change; in Fig.9a this depth is plotted together with the mean depth position of the juvenile and adult layer. It is clear that juveniles fill up their stomachs in the crepuscular periods, as encounter rate exceeds the stomach evacuation rate, while at daytime feeding is encounter limited. Digestion limitation during the crepuscular periods results in a portion of the encountered prey items not being ingested. The amount of food
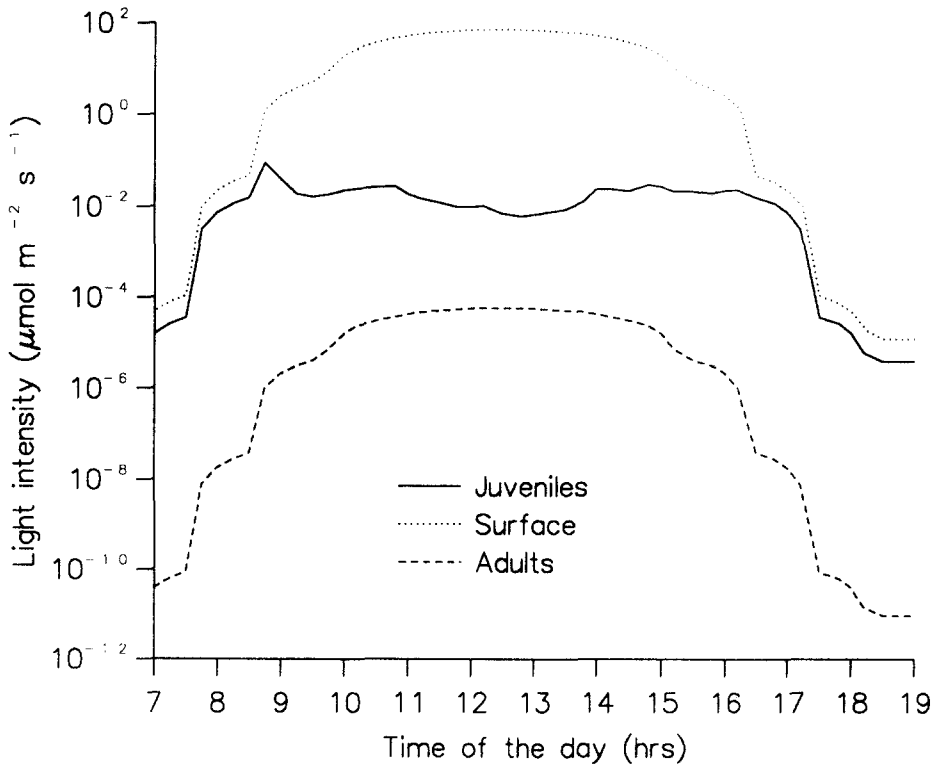

FIG.7. Light intensity (μmol m^{-2}s^{-1}) at the surface and in the juvenile and adult layers.

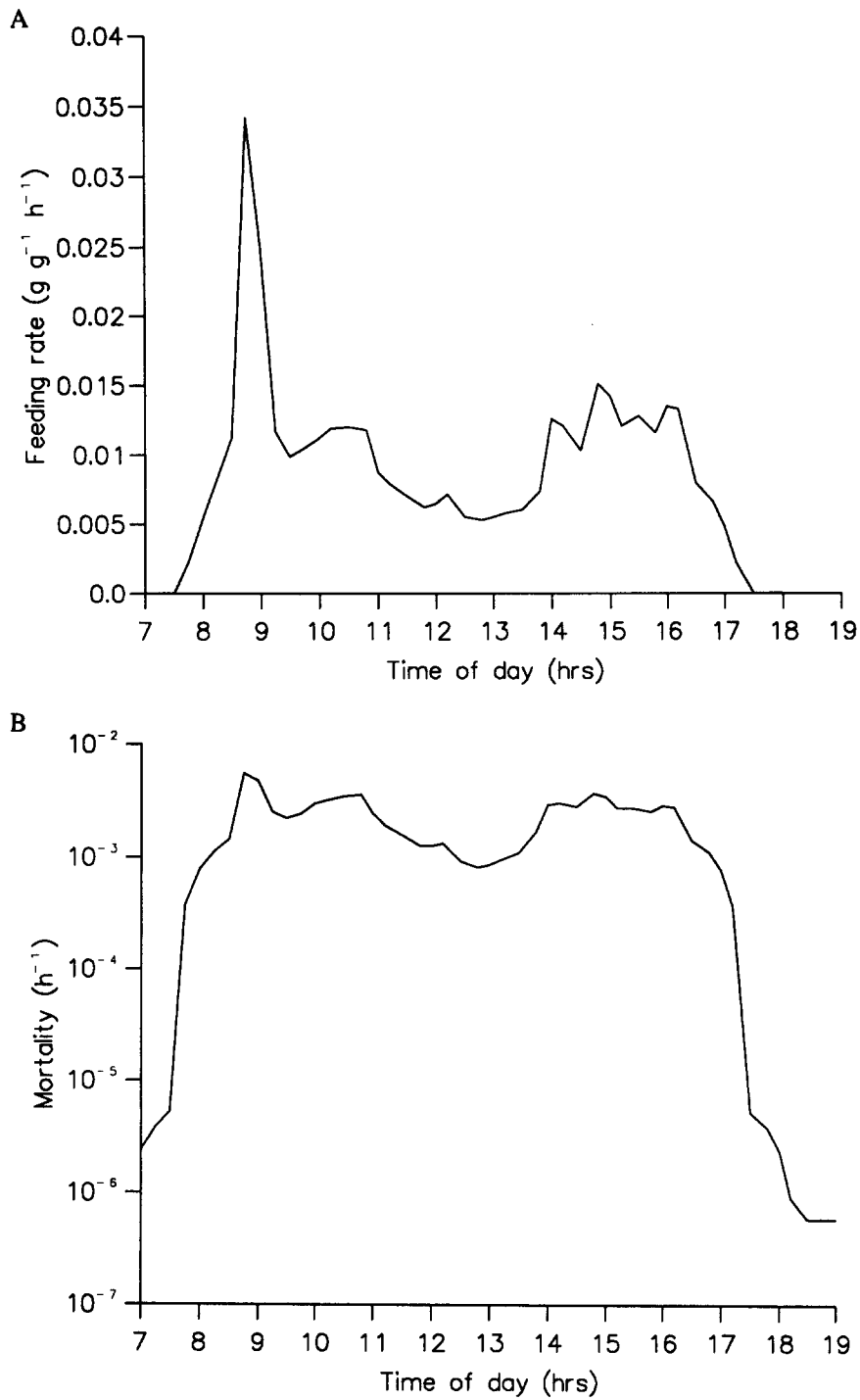FIG.8. Daytime pattern in (A) average feeding rate (f, g g⁻¹h⁻¹) and (B) average mortality risk
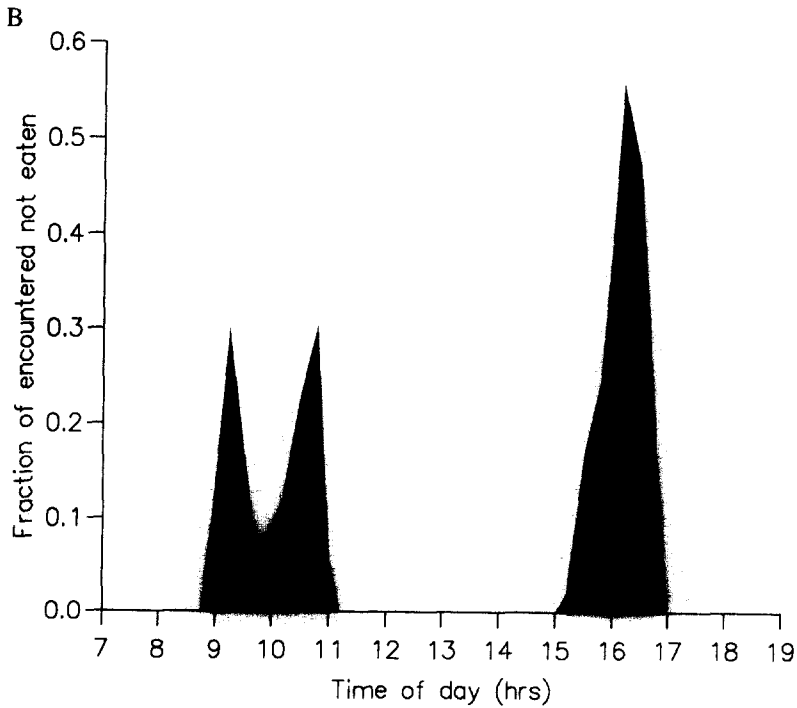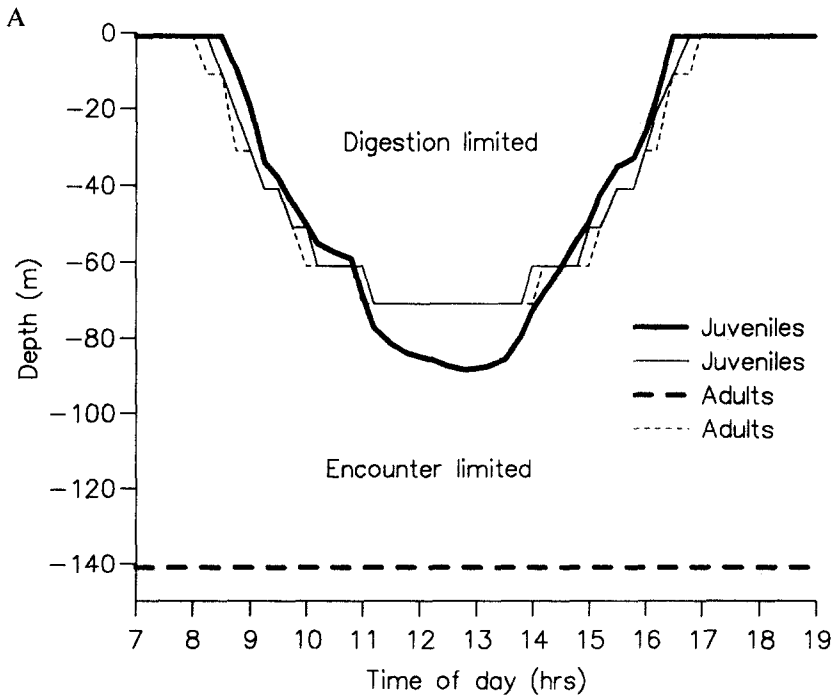(M, h⁻¹) for juveniles in basic run.

FIG.9. (A) Mean depth (thick lines) of juvenile and adult fish. Thin lines mark the depths where feeding rate shifts from digestion to encounter limitation. (B) Fraction of food encountered by juvenile fish in the different time intervals which is not eaten as a result stomach limitation.
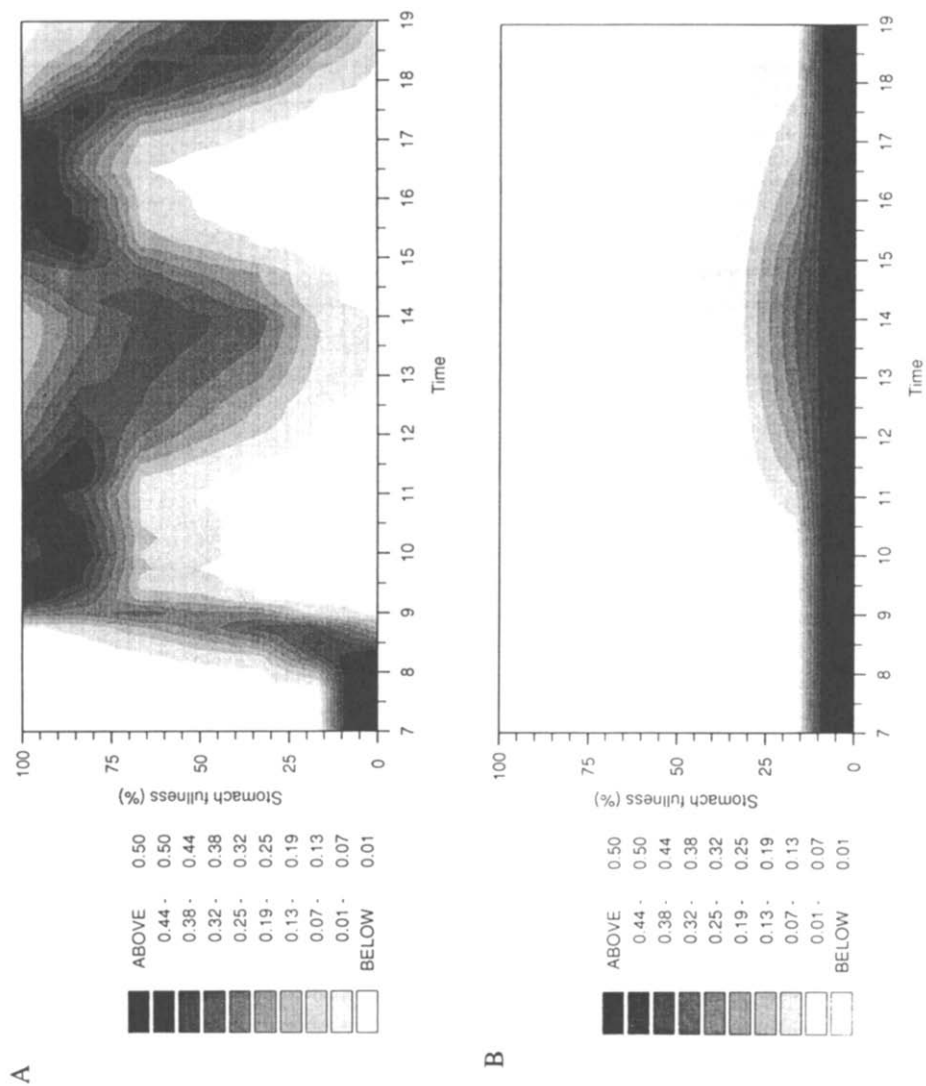
Fig. 10. Stomach fullness (% of maximum capacity) of juveniles (A) and adults (B) in the basic run. The scale to the left indicates fractions of fish at different stomach fullness.
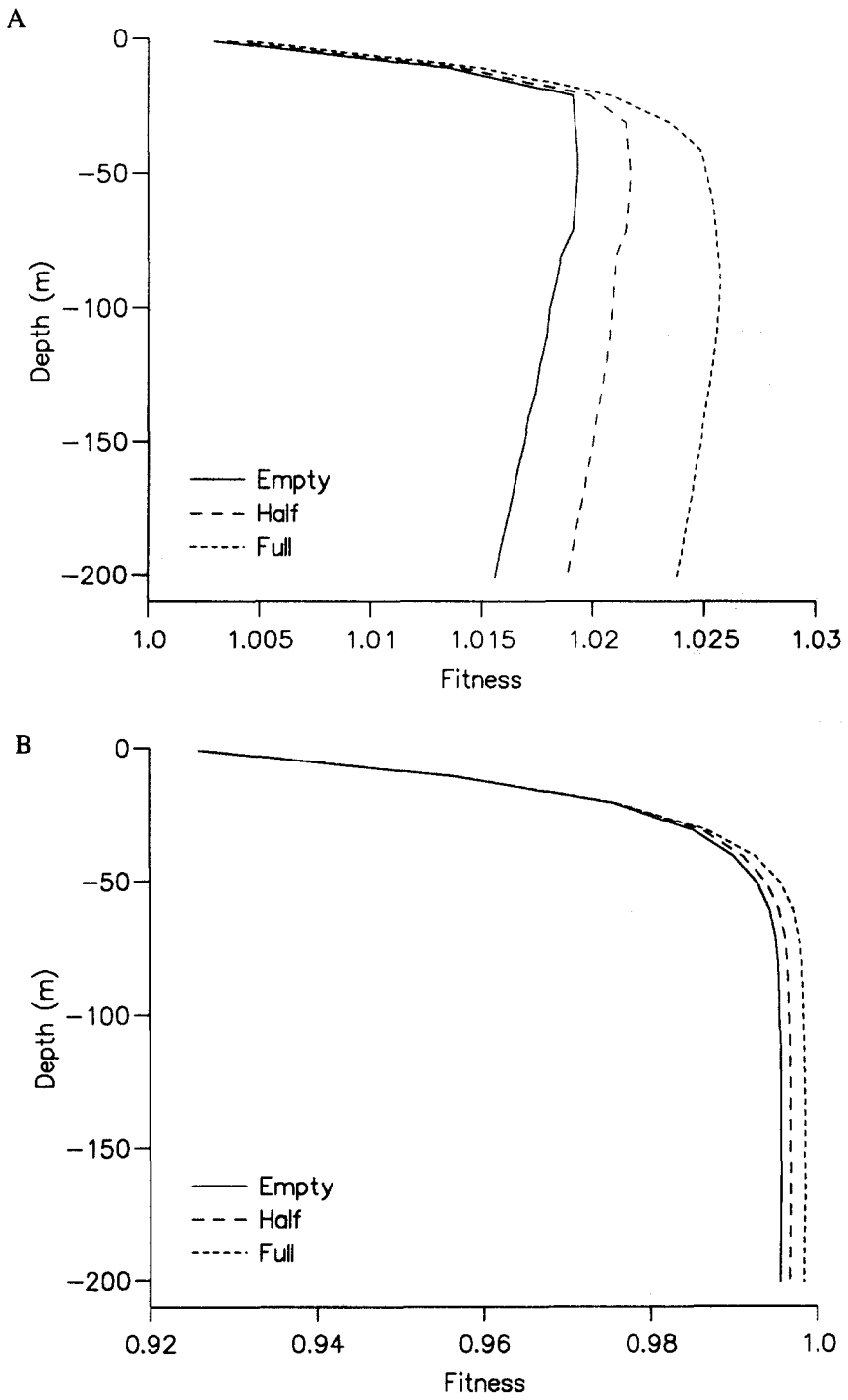
FIG.11. (A) Fitness-depth relations at midday for juvenile fish with empty, half full and full stomach.
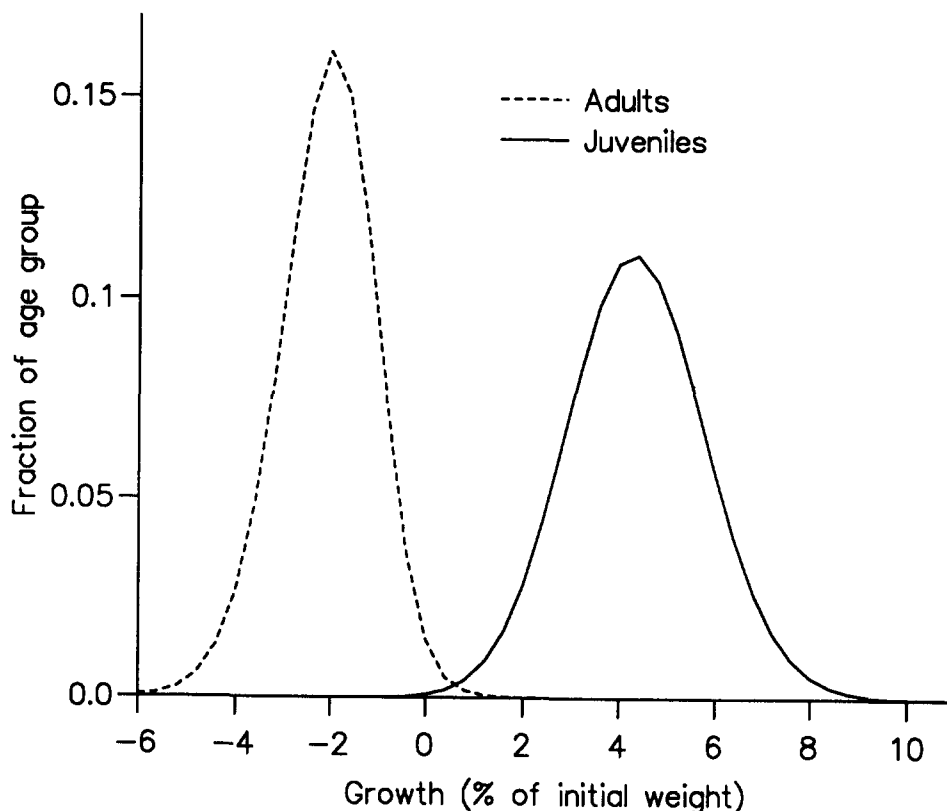(B) Fitness-depth relations at midday for adult fish with empty, half full and full stomach.

FIG.12. Growth distribution in juvenile and adult fish at the terminal time. Growth is given as percentage weight change relative to the initial weight

encountered not ingested is plotted as fractions of the total food encountered in the different time intervals (Fig.9b). At dusk as much as 60% is not ingested, while at dawn about 30% is not ingested. The stomach fullness (%) of individuals in the juvenile layer during the diel cycle is given in Fig.10a, showing that maximum degree of fullness occurs in the crepuscular periods. At night feeding ceases, and stomach contents decrease according to the stomach evacuation rate.

Optimal depth position changes with the degree of stomach fullness since feeding potential changes with the stomach capacity (Δs in Eq.8). The depth-fitness relations at midday (1230h) for fish with empty, half full and full stomach is given in Fig.11. There is a 50m difference in the optimal depth position for fish with empty and full stomachs.

The growth distribution of juveniles at the final time (terminal time) is given as percentage weight increase in Fig.12, and average growth rate obtained for juveniles is 0.043g $g^{-1}d^{-1}$ and mortality rate is 0.021d^{-1} (Table 4).

The adult layer remains static at 141m throughout the diel cycle (Fig.6); consequently feeding (Fig.13a) and mortality rates (Fig.13b) vary according to surface light intensity (Fig.7) which is
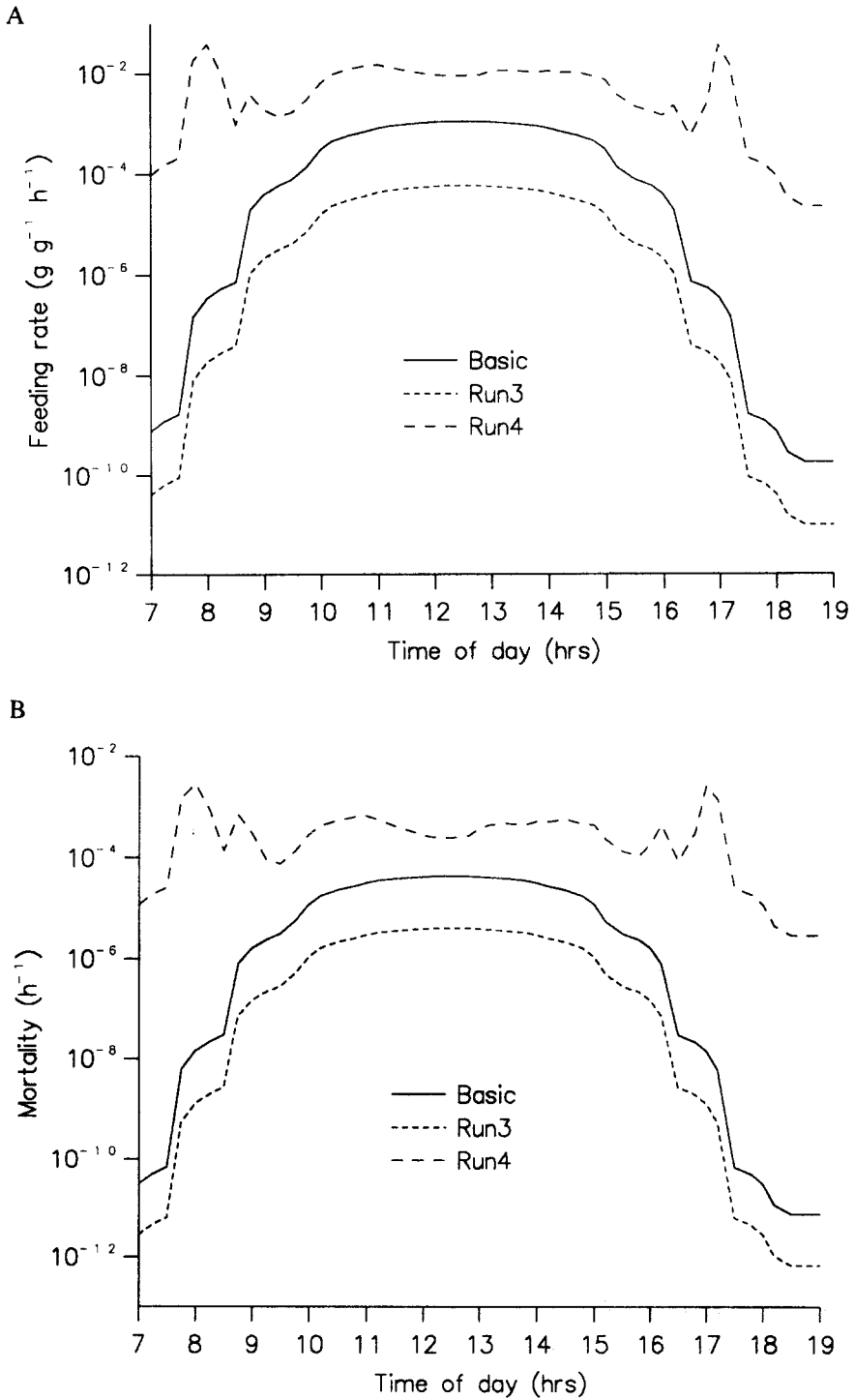
A

B

FIG.13. Average feeding rate (g g⁻¹h⁻¹) (A) and mortality (h⁻¹) (B) of adult fish in basic run, increased (run 4) and reduced (run 3) prey individual mass.

maximum at midday (Fig.7, Table 4). Feeding rate in the adult layer is constantly limited by visual prey encounter rate (Fig.9a) and therefore stomach contents are constantly low (Fig.10b). In contrast to juveniles the stomach contents of adults have no effect on their optimal depth position (Fig.11). The terminal growth distribution of adults is given in Fig.12, and the average growth rate is negative (-0.021g g^{-1}d^{-1}) and average mortality rate is only 1.8 10^{-4}d^{-1} (Table 4).

3.2 Changing the relation between predation risk and prey encounter rate

If the prey encounter rate is reduced by either prey density (run 1) or the prey mass (run 3) the tendency towards crepuscular intensified feeding within the juvenile layer is increased. The descent from surface at dawn is delayed, the surface ascent at dusk is advanced and the fish move deeper during daytime. The differences in feeding rate (Fig.14a) and mortality (Fig.14b) between crepuscular (especially dusk) and daytime levels increase relative to the basic run, and the deeper daytime position combined with reduced prey encounter rate gives a strongly encounter limited feeding rate during daytime (Table 4).

The changes in stomach contents are plotted against time in Fig.15, the decrease in stomach contents after dawn reflects the strong encounter-limitation on feeding during daytime. The average depth position of juveniles, for the run with reduced prey size (run 3) is plotted with the depth where feeding shifts from digestion limitation to encounter limitation (Fig.16). The lowering stomach contents towards dusk leads to a higher feeding potential, thus feeding at dusk reaches about the same level as at dawn. Both diel growth and mortality are reduced (Table 4) in the runs with decreased encounter probability (runs 1 and 3).

Increasing the encounter rate by increasing prey density (run 2) and prey size (run 4) results in earlier surface descent at dawn and delayed surface ascent at dusk. Daytime depth position is deeper for increased prey size, while increased prey density gives a shallower daytime position relative to the basic run (Table 4). Mortality (Fig.14b) is reduced in the crepuscular periods (and during daytime for run 4) as a result of reduced light intensity. However, as prey encounter is enhanced, the crepuscular feeding rate is at about the same level as in the basic run (Fig.14a) even though light intensity is less (Table 4), and the daytime feeding is about twice the basic level. This gives an increased diel growth rate at a lower expense of mortality (Table 4).

Changing the predation risk (runs 5 and 6) generally gives the same overall changes as does varying of the encounter rate. Thus increasing predation gives bimodal crepuscular feeding (Fig.17a) and mortality patterns (Fig.17b), with deeper daytime depth positions (Table 4). Reducing the predation risk smooths out the differences between crepuscular and daytime feeding and mortality (Fig.17) with a shallower daytime position (Table 4).

The adult layer responds to reductions in prey encounter rate and increased predation risk by staying deeper (Table 4), but still with a static depth distribution. As for juveniles, feeding and mortality decrease relative to the basic run (Fig.13a, Table 4).

Increased prey mass (run 4) induces vertical migration in the adult layer, and they migrate to and from surface at dusk and dawn to daytime depths of 118m (Table 4). Feeding rates (Fig.13a) and mortality (Fig.13b) have maxima during the crepuscular periods which are about 4 times the daytime levels, and feeding rate is limited by stomach evacuation rate during the day in run 4 (Table 4). Increased prey density does not affect the adult distribution, but feeding rate increases and the negative growth is reduced (Table 4).
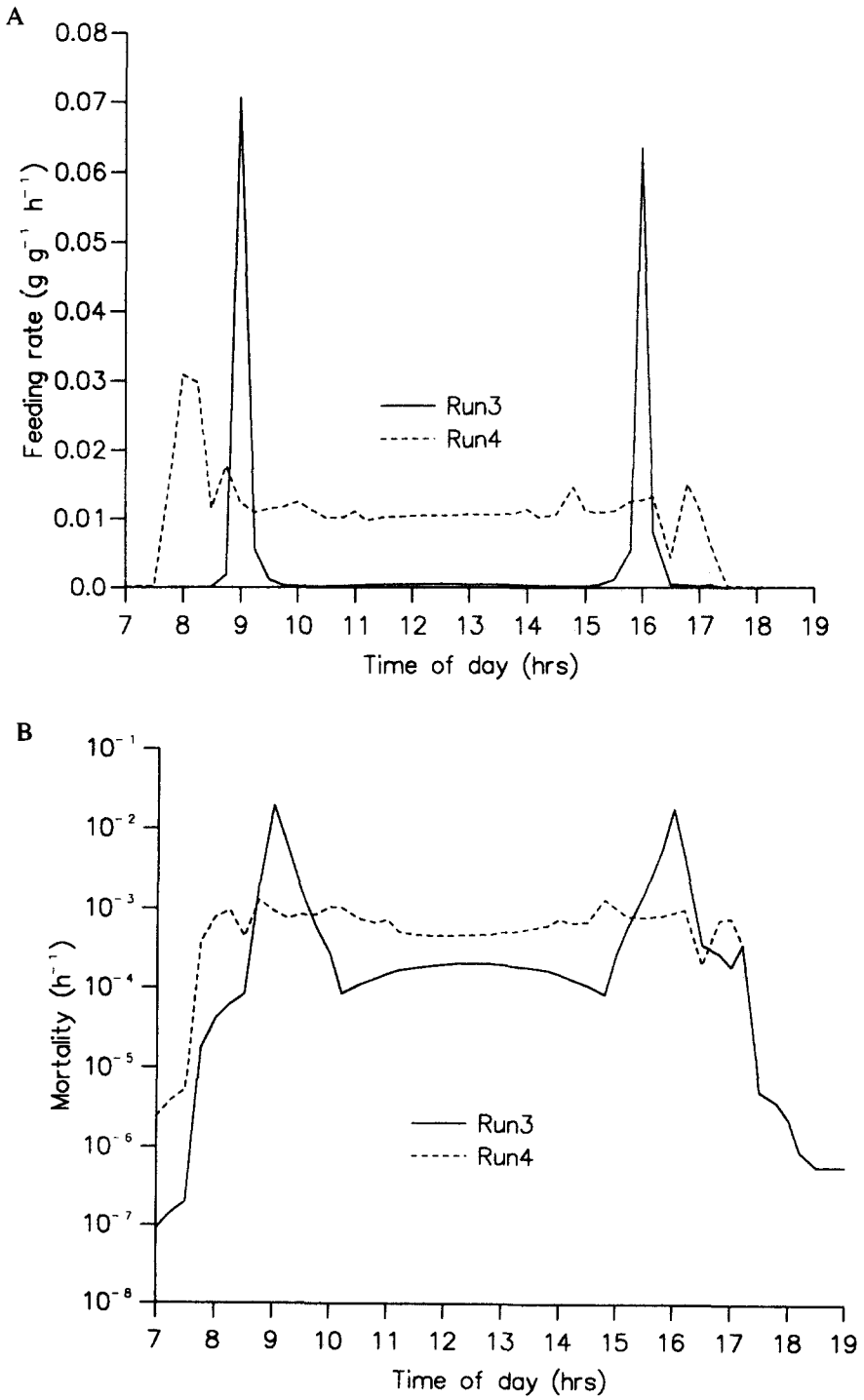
FIG. 14. Average feeding rate (g g^{-1}h^{-1}) (A) and mortality (h^{-1}) (B) for juveniles at increased (run 4) and reduced (run 3) prey individual mass.
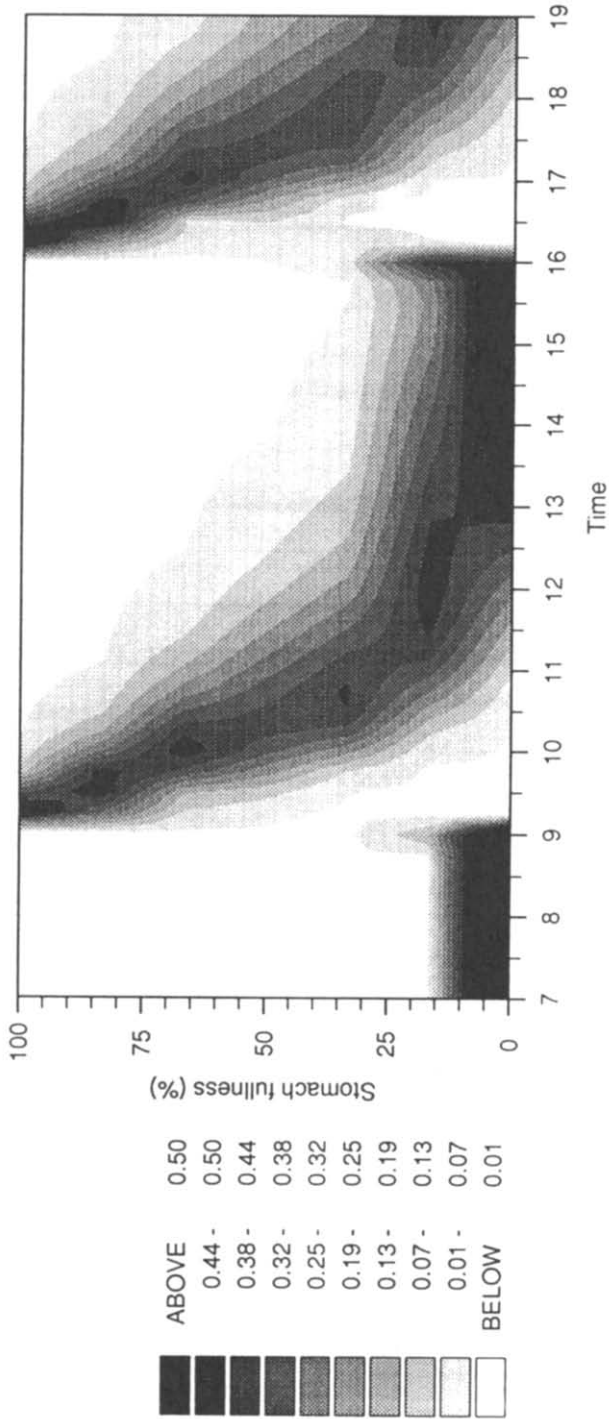
FIG.15. Stomach fullness (% of maximum capacity) of the juvenile layer when prey mass is reduced (run 3). The scale to the left indicates percent of fish at different stomach fullness.
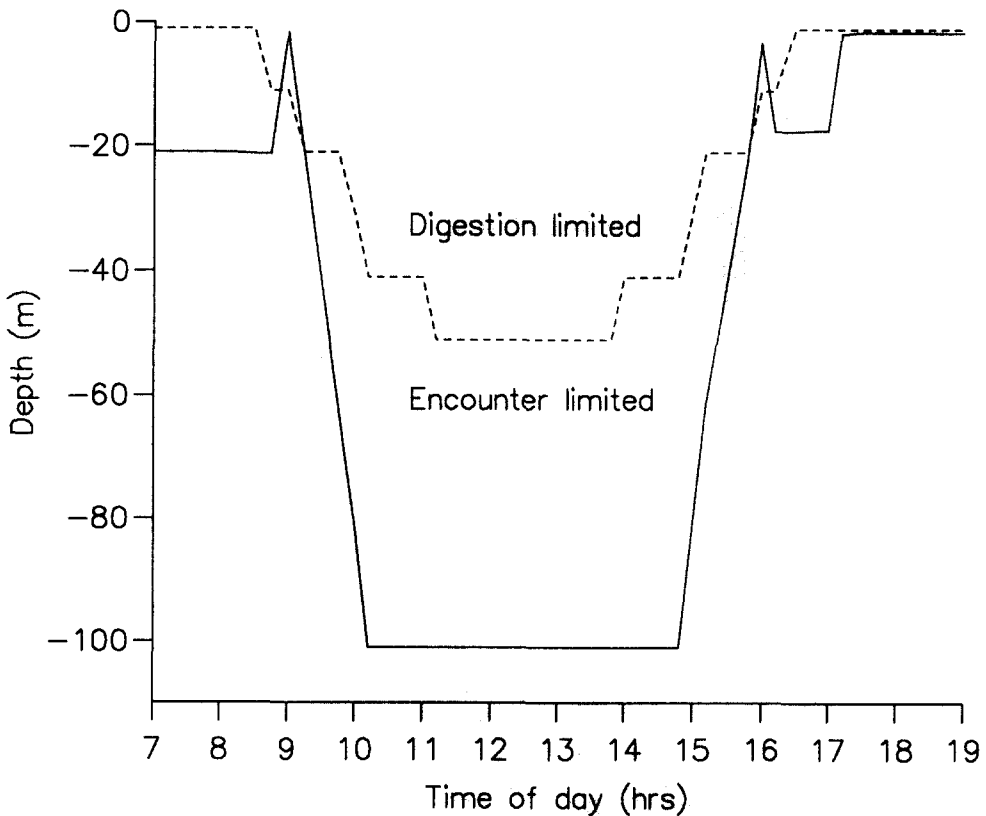
FIG. 16. Mean depth of the juvenile layer when prey individual mass is reduced (run 3). Broken line mark the depth where feeding rate shifts between digestion and prey encounter limitation.

3.3 Changing surface light

Changes in the surface light have influence on both predation risk and prey encounter rate throughout the depth range. Reducing surface light (run 7) reduces the daytime depth position of the juvenile layer to 40m (Table 4). The temperature is higher at 40m relative to 90-100m (Fig.3b), and stomach evacuation and potential feeding rate increase relative to the basic run. This results in a higher optimal light regime during daytime (Table 4) with approximately a doubling of the feeding (Fig.18a) and mortality rate (Fig.18b), resulting in an increase in both diel growth and mortality.

Increased surface light deepens the juvenile layer at 110m during the day (Table 4). Light intensity (Table 4) and mortality in the layer are lower in the daytime (Fig.18b), but feeding rate is about twice the basic level (Fig.18a), though light intensities are reduced. The reason for this is that prey size increases below 75m, which also increases the food value per prey item encountered at 110m relative to 86m (in the basic run). Thus diel growth rate is about equal to the basic run while mortality is almost halved (Table 4).

The adult position remains static at 151m when light intensities are reduced, which unexpectedly is 10m deeper than in the basic run (Table 4). The shift in depth preference induced by light reduction results from changes in the relation between the mortality risk and encounter rate. The
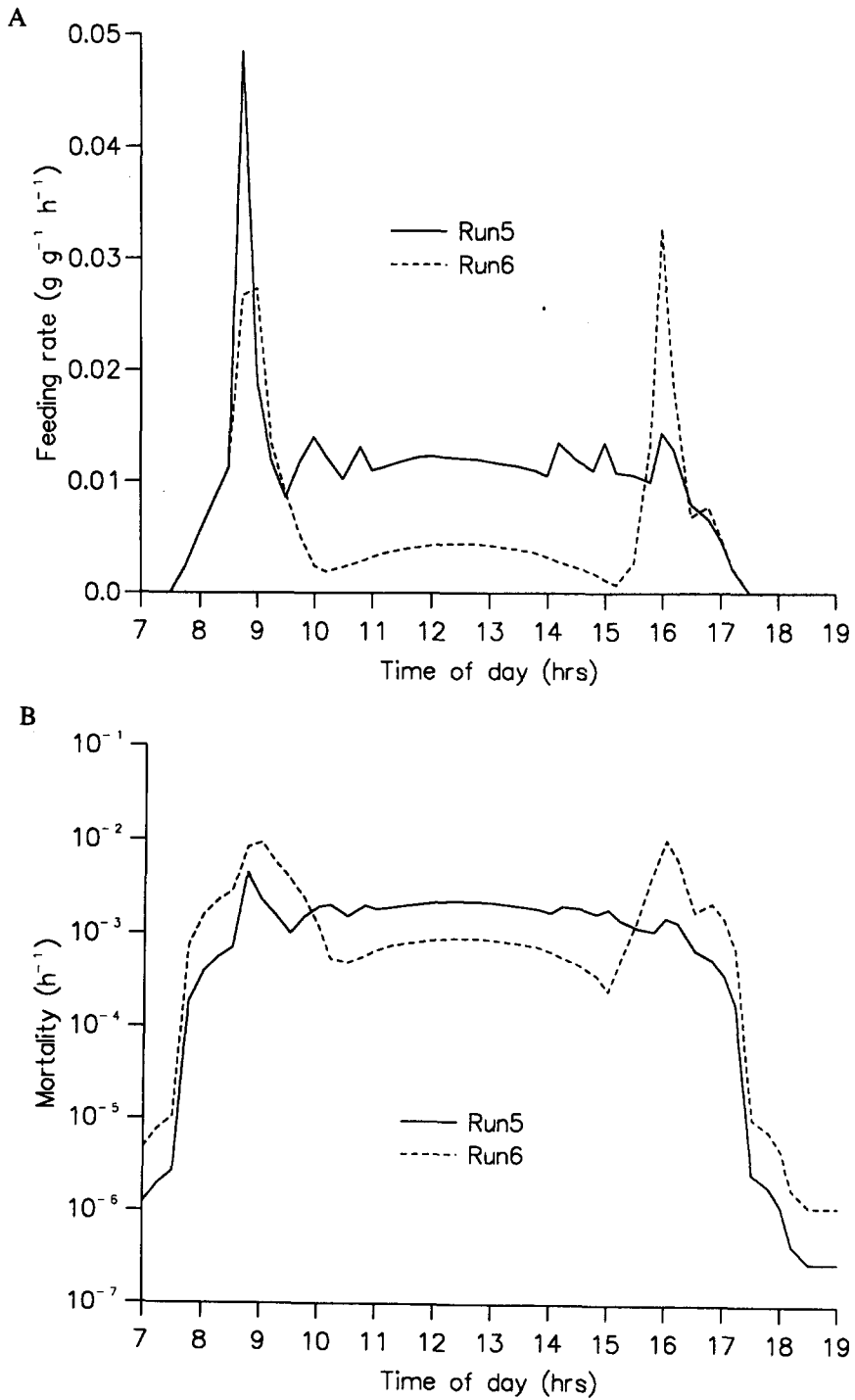
FIG.17. Average feeding rate (g g^{-1}h^{-1}) (A) and mortality rate (h^{-1}) (B) of juveniles for increased (run 6) and reduced (run 5) mortality risk.
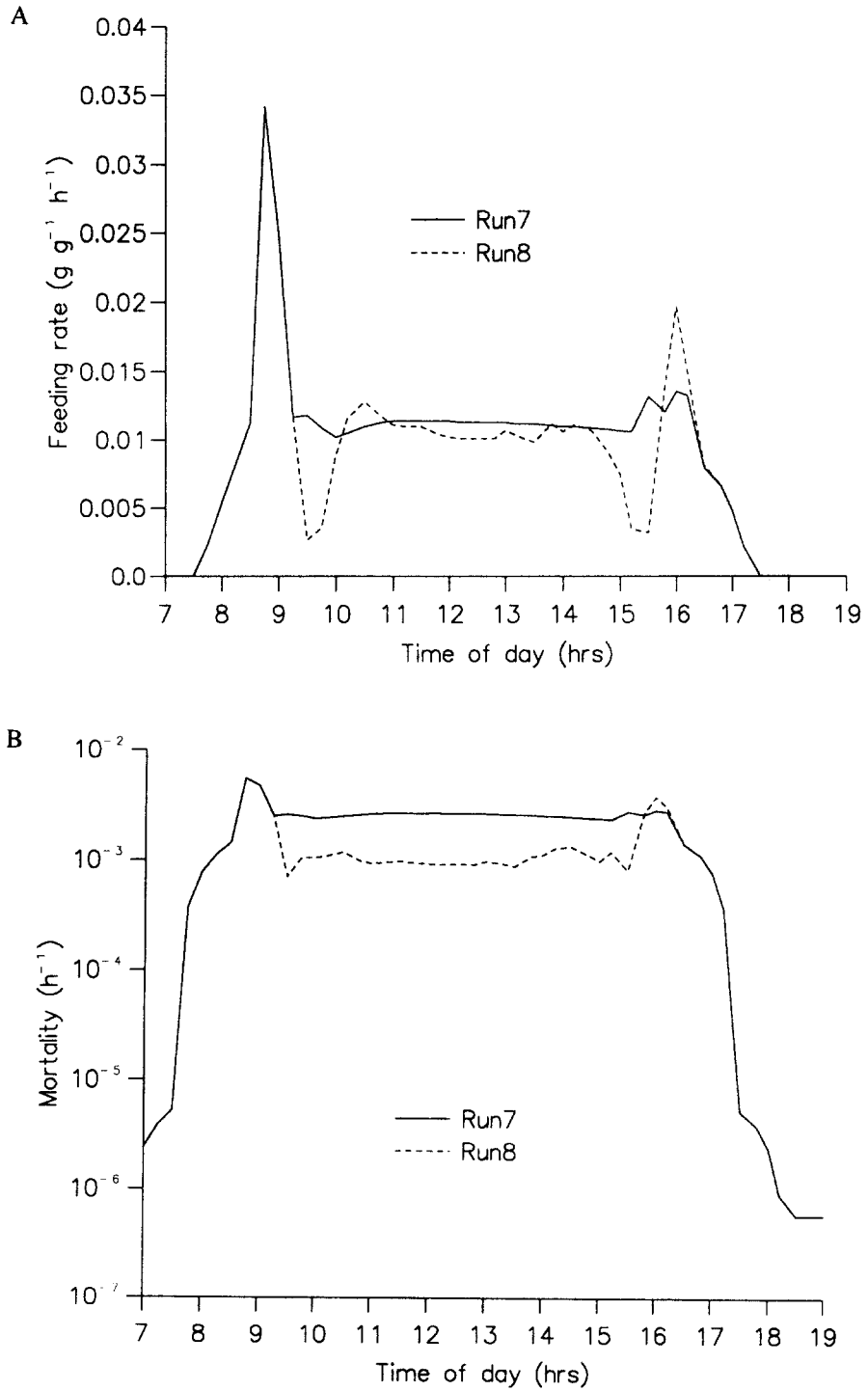
FIG.18. Average feeding rate (g g⁻¹h⁻¹) (A) and mortality (h⁻¹) (B) of juvenile fish for reduced (run 7) and increased (run 8) surface light intensity.

encounter rate decreases more than mortality risk, and the adults compensate for this effect by moving to 151m (larger prey at higher density) maintaining the optimal ratio between predation risk and ingestion rate (M/F_m, Fig.5b). The reduced light intensity (Table 4) combined with a deeper position reduces both mortality rate and feeding rate compared with the basic run (Table 4).

Increasing surface light gives similar adult distributions as in the basic run (Table 4), however with a slight response at midday, where a small proportion (<0.1) moves to 151m. A large increase in surface light results in a positive growth rate and a 10-fold increase in mortality and feeding rate relative to the basic run (Table 4).

3.4 Changing temperature

Increased temperature gives a daytime depth at 70m for the juvenile layer, resulting in higher light intensity (Table 4), mortality and feeding rates during daytime. This increase in optimal light intensity results from the higher temperature which increases the stomach evacuation and feeding potential. The increased temperature also increases the metabolic costs, but the overall effect is to increase diel growth rate (Table 4).

Reduced temperature has the opposite effect with deeper daytime position (Table 4) and reduced feeding – and mortality rates during daytime. The resulting diel growth and mortality rates are lower than in the basic run (Table 4). Temperature changes give the same adult depth distribution as the basic run, but decreased temperature reduces the negative growth rate because of the reduced metabolic costs (Table 4).

3.5 Changing stomach evacuation rate

Increasing the stomach evacuation rate increases the feeding potential, and the juvenile layer stays at a shallower depth (Table 4) with higher feeding and mortality rates during daytime (similar to increasing the temperature in run 10). Reduction of the stomach evacuation rate has the opposite effect. Both the daytime mortality and feeding rates fall relative to the basic run.

Variations in the stomach evacuation rate has no influence on either distribution (Table 4) or growth of the adult layer. As the feeding rate of adults is strongly limited by the prey encounter rate, variation of the stomach evacuation rate has no effect since there is little to be evacuated.

3.6 Changing the terminal fitness function for juveniles

Increasing the steepness of the fitness function gives a 25m shallower daytime depth for the juvenile layer where light intensity (Table 4) and feeding and mortality rates are increased. This increase in tolerance to mortality results from the increase in the benefits gained by feeding (terminal fitness) and the daily growth and mortality increase relative to the basic run (Table 4).

Decreasing the steepness of the fitness function to about adult level maintains the juvenile layer depth at 102m with surface migration at night (Table 4). This results in negative growth rate but reduces mortality to only 4% of the basic level, comparable to adult strategy. However, as predation risk and feeding relate differently for juveniles and adults (Fig.5a), the optimal depth positions are different for the two age groups although the terminal fitness functions are at the same level.
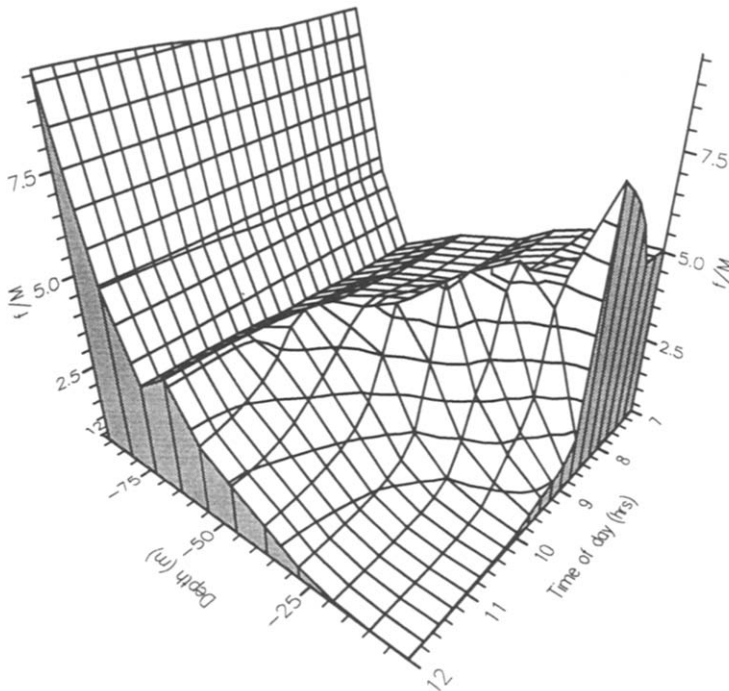
FIG.19. Feeding rate (g g⁻¹h⁻¹) over mortality risk (h⁻¹) for a situation with empty stomach
(i.e. maximum capacity).

3.7 Doubling the time horizon

The time perspective was increased to 48h to see if the increasing time from the terminal reward function would alter the optimal policy of the fishes. The predictions seem identical to the basic run (24h) with juvenile and adult growth rates of 0.0428 and -0.0211g g⁻¹d⁻¹ respectively and mortalities of 2.1 10⁻² and 1.8 10⁻⁴d⁻¹ for juveniles and adults respectively. The vertical distribution for this run is given in Fig.20.

4. DISCUSSION

The model predictions seem to give a relatively good picture of the vertical distributions and feeding patterns observed in Masfjorden in January (GISKE, AKSNES, BALIÑO, KAARTVEDT, LIE, NORDEIDE, SALVANES, WAKILI and AADNESEN, 1990; GISKE and AKSNES, 1992). A problem in making direct comparisons between predictions and observations is the large variability in the natural surface light during the day whereas the model light intensity regime is smooth and regular. Therefore, comparing the general trends in the observed depth distributions and feeding rates with the model predictions is probably a better validation for the model rather than direct depth-time correlations with nature.
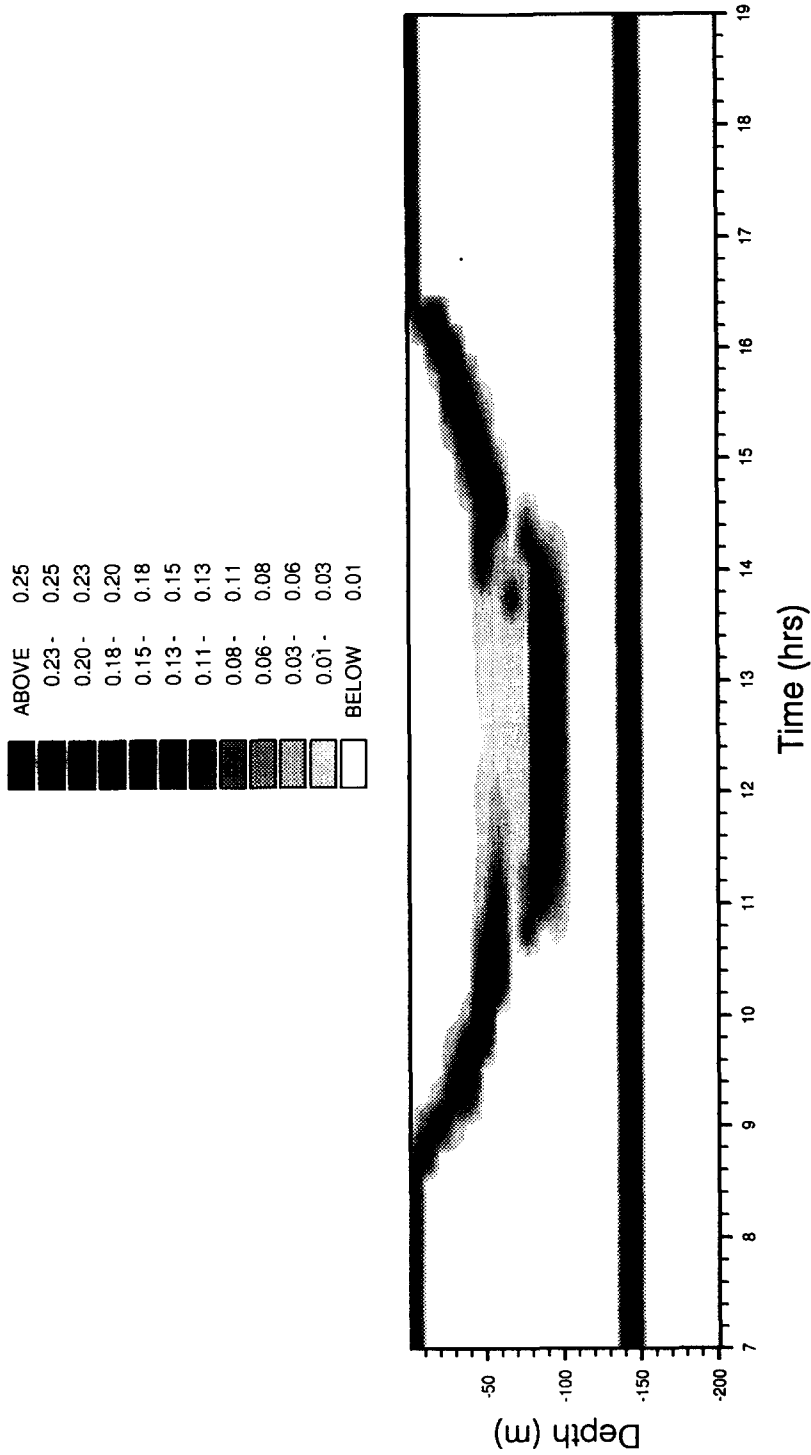
FIG.20. Diel vertical distribution of juveniles (upper layer) and adults (lower layer) when time horizon is doubled (48h). The plot presents the distribution the first day of the model period. The scale at the top indicates the fraction of the population at each depth.

4.1 Vertical distribution

The most striking difference between model predictions and observations is the night distribution of the juvenile layer, for which observations (Fig.1) show the layer at the depth of the temperature maximum at 40-60m, whereas the model predicts a surface position. The surface light intensities at night in winter are probably insufficient for visual feeding, and the risk from visual predation is also likely to be very low during the night. Temperature is, therefore, probably the dominant factor controlling depth distribution during the night. Moreover, if digestion times in the cold surface water exceed the duration of the night, the growth rate becomes limited by the digestive processes. Then the advantage of staying in the temperature maximum at night may be through increasing the metabolic conversion rate, and thereby increasing the growth. This strategy has also been observed in juvenile sockeye salmon (LEVY, 1990) and juvenile sculpins (WURTZBAUGH and NEVERMAN, 1988). The digestive processes (in terms of food processing rates and capacity) in this model are only represented by the stomach variable as the 'growth' variable (w) only trace the mass budget (mass evacuated from stomach - mass lost in metabolism). Thus if stomach emptying time in the cold surface water is shorter than the night, it is optimal for the model fish to stay in the cold surface water in order to minimize the metabolic costs, thereby maximizing net growth. The omission of how gut processing time and biochemical processes might be influenced by temperature may explain why the model fails to give a correct night time distribution of the juveniles.

Another distinct difference between predictions and observations is the static depth distribution of adult (model) fish with no response to variations in surface light; observations indicate that light responses occur at dawn and dusk (Fig.1) and there are also responses to instantaneous changes in light during the daytime (BALIÑO and AKSNES, 1993). The depth of the modelled adult layer is also slightly deeper than is observed during daytime.

The sound scattering layers from Masfjorden indicate a vertical range of the two layers about 20-30m with some variation throughout the diel cycle (GISKE, AKSNES, BALIÑO, KAARTVEDT, LIE, NORDEIDE, SALVANES, WAKILI and AADNESEN, 1990). This observed dispersion may result from adjustments to light intensity, for example hungry fish may seek the upper part of the layer in order to increase the prey encounter rate, but when satiated may move down to the lower and darker part of the layer where their visibility to predators is lower. Such individual differences, caused by different levels of hunger, was also observed within shoals of herring by ROBINSON and PITCHER (1989a,b). Vertical dispersion of fish may also result from space limitation and competition between individuals. The model is capable of predicting the vertical dispersion resulting from variations in state dependent depth choice (i.e. hunger and satiation, Figs 6 and 11). However, space limiting factors are not included as optimal depth is calculated in a back iteration procedure, and is computed without knowledge of the positions of other individuals.

4.2 Feeding patterns

The predicted feeding pattern of juveniles closely matches the observed pattern, with relatively high feeding rates throughout the day which increase during the crepuscular periods. Stomach analyses showed that around midday 85% of the juveniles had more than half full stomachs (GISKE and AKSNES, 1992) while most adults had very little in their stomachs throughout the day with a maximum around midday (GISKE, AKSNES, BALIÑO, KAARTVEDT, LIE, NORDEIDE, SALVANES, WAKILI and AADNESEN, 1990).

GISKE and AKSNES (1992) applied the same visual model and field data (light and zooplankton distribution) to calculate the feeding and growth of juveniles and adults in the two sound scattering

layers. They found the same pattern of variation in feeding rates throughout the day, with intensified feeding in the crepuscular periods as described here. They estimated ratios of 10:1 between dawn:daytime feeding and 3:1 between dusk:daytime feeding compared with the ratios obtained here (in the basic run) of about 7:1 (dawn:daytime) and 2:1 (dusk:daytime).

4.3 Trade-offs involved in crepuscular feeding

One of the replicated characteristics of most runs is the movement of the juvenile layer to the surface at dawn and dusk, similar to CLARK and LEVY (1988) and MASON and PATRICK (1993). CLARK and LEVY (1988) concluded that this behaviour extends the periods of daylight and thereby prolongs the period of potential feeding.

Feeding rate is generally higher during the crepuscular periods than during the rest of the day, particularly at dawn when the fish start with empty stomachs (no feeding opportunity at night). The reduced stomach fullness at dusk also explains the intensified feeding rate in this interval. The question that arises is why the feeding rate falls to a level that is insufficient to compensate for the stomach evacuation rate during the day.

The trend towards a crepuscular feeding pattern becomes more prominent as the M/F_m ratio is increased (runs 1,3,6) and feeding almost ceases during daytime in these runs. In high risk environments it seems optimal to restrict feeding to dawn and dusk, and devote daytime to predator avoidance. Why this is the optimal strategy can be explained from the depth profiles of predation risk and encounter rate (M and e) (Fig.5a), and the ratio between predation risk and prey mass ingestion rate (M/F_m) throughout the depth column (Fig.5b). From these figures it is clear that the optimal depths, with respect to feeding and mortality, are located near the surface and at the depth zone from 150-200m. The reduced M/F_m ratio in the surface results from increased water turbidity, which reduces the predator's long visual range relatively more than the short visual range of *M. muelleri*. In the 150m zone the M/F_m reduction results from increased prey mass and density, thereby increasing the mass encounter rate of *M. muelleri* relative to predation risk. However, as the 150m zone never provides sufficient light for efficient feeding, the surface water is the only alternative to combine efficient feeding with low predation. Thus, when fish enter the surface with empty stomachs in the crepuscular periods, they can ingest a maximum of food in a 'low risk' environment. Alternatively, if the fish stayed at higher light intensities throughout the day, although they would increase their feeding rate, the increased predation would make this strategy sub-optimal compared to the 'crepuscular' strategy. This is illustrated in Table 5 where the fish were constrained to sub-optimal depths throughout the diel cycle, ranging from 20m below and above the optimum. Feeding rate over predation risk (f/M) is plotted against time (0730-1230h) and depth (0-100m zone) in Fig.19 for a situation with empty stomach (i.e. maximal stomach capacity). The figure illustrates the point discussed above, and as long as the prey encounters do not exceed the stomach capacity, the surface provides the best opportunity for 'low mortality' feeding (see GISKE, AKSNES and FIKSEN, 1993, for a more detailed discussion of this phenomenon). This is probably the most important mechanism underlying the preference for crepuscular surface feeding in the model. The tendency towards dawn-dusk feeding is, however, very dependent on the M/F_m ratio, and at low ratios (runs 2, 4 and 5) the feeding rate seems to be evenly distributed between daytime and dusk (dawn is always high because of empty stomachs).

TABLE 5. Deviations in diel feeding rates, mortality rates and fitness (terminal fitness multiplied by survival probability) for sub-optimal depth positions throughout the diel cycle (using parameter values from basic run). Fish were forced into positions shallower or deeper than the optimal depth position in basic run.

| Depth deviation from basic run | Juveniles | | | Adults | | |
	f (g g^{-1}d^{-1})	M (d^{-1})	Fitness	f (g g^{-1}d^{-1})	m (d^{-1})	Fitness
20m shallower	0.1076	.0491	0.9856	0.0048	.000867	0.9950
10m shallower	0.1048	.0300	1.0032	0.0047	.000393	0.9954
Basic run	0.0985	.0210	1.0092	0.0044	.000178	0.9956
10m deeper	0.0775	.0187	0.9983	0.0034	.000080	0.9956
20m deeper	0.0502	.0139	0.9908	0.0023	.000036	0.9955

A natural mechanism that may also contribute to intensified crepuscular feeding, is the link between stomach fullness and hunger response. After dawn feeding the fish becomes satiated, and lose their motivation to feed. During the day they then give priority to anti-predator behaviour rather than to feeding, so by dusk their stomachs are again empty, and hunger motivates them to start feeding again. However, observations indicate that the fish are feeding actively throughout the day, and do not cease completely (GISKE, AKSNES, BALIÑO, KAARTVEDT, LIE, NORDEIDE, SALVANES, WAKILI and AADNESEN, 1990; GISKE and AKSNES, 1992). The response to instantaneous changes of the light intensity also support the idea that the fish adjusts to light regimes where feeding is possible.

4.4 Stochastic versus deterministic feeding

Foraging success is determined by uncertain and stochastic processes in the environment (CLARK and MANGEL, 1986) so foraging is probably best represented by stochastic models (STEPHENS and CHARNOV, 1982). The use of both deterministic and stochastic models often produces different predictions of optimal strategy (CARACO, 1980). An interesting result from the model is how the juvenile layer adjusts to light intensity and prey encounter rate throughout the day. From a deterministic point of view, the expected depth position should be either at or below a depth where prey encounter rate exactly compensates the stomach capacity. The depths obtained, however, indicate a prey encounter rate that far exceeds the stomach capacity in the crepuscular periods (Fig.9b); for those runs in which prey encounter rates were enhanced the juveniles stayed at depths where the prey encounter rate exceeded stomach capacity throughout the day. This is a result of the probability functions (Poisson) of the model, and high prey encounter rates (resulting in high encounter expectations) is a way of maximizing feeding probability (i.e. if encounter expectation exactly compensates the stomach capacity this would result in a 50% chance of falling below the stomach compensation level).

GISKE and AKSNES (1992) also estimated encounter rates that exceeded the stomach capacity in the crepuscular periods, and suggested that they had underestimated the stomach capacity; it might just be that juveniles enter such high light intensities in order to ensure they fill their stomachs.

4.5 The adult strategy

The deep and static distribution of the adult layer result from the low fitness gain from feeding, and therefore a low tolerance to mortality (cf clutch manipulators defined by AKSNES and GISKE,

1990). Below 120m both prey density and prey size increase strongly and result in a large reduction in the M/F$_m$ ratio below 120m (Fig.5b). If adults migrated towards the 100m zone during the crepuscular periods, as observed in Masfjorden (GISKE, AKSNES, BALIÑO, KAARTVEDT, LIE, NORDEIDE, SALVANES, WAKILI and AADNESEN, 1990), they would increase their daily food intake, but the risk of predation would increase relatively more and result in a large deleterious shift in the optimal M/F$_m$ balance (defined by the terminal fitness function).

This raises a question about the simplistic zooplankton representation used in the model, where neither fine scale variations of the zooplankton densities nor the variability of the prey biomass at each depth are detected. Field data from Masfjorden (BALIÑO and AKSNES, 1993) indicate that most zooplankton groups have a static diel distribution, although migration occurs in some groups (KAARTVEDT, AKSNES and AADNESEN, 1988). Vertical movements of zooplankton have also been reported (LIE, MAGNESEN, TUNBERG and AKSNES, 1983; MAGNESEN, AKSNES and SKJOLDAL, 1989) from the nearby fjord Lindåspollene. Thus if adult fish stay within high density layers of zooplankton, movements of these layers may explain the observed movements of adult fish.

Though the observational data may lack the fine scale variations in the zooplankton depth profiles and possible day-night variations, they do reveal a large gross scale difference in zooplankton density and size between the 0-100m zone and the 100-200m zone. Thus we believe that the main conclusion on adult depth preferences is not affected by fine scale imprecisions of the zooplankton data.

4.6 Seasonal trade-offs

The stable depth distribution of the adults occurs only in the winter months, and they perform vertical migration the rest of the year. With the prevailing environmental conditions during winter, the optimal strategy for adults seems to be tolerating a short period of low or even negative growth, since the fitness reward gained from positive growth is more than offset by the increase in mortality risk. It is important to bear in mind that our assumptions of negative growth rate for adult fish are based on stomach analysis and vague estimates of metabolic requirements (from literature on other fish species), and perhaps are they balancing feeding rate vs metabolic requirements. Whether adult fish have negative or neutral growth is really of minor importance as long as the main issue is the difference between juvenile and adult feeding-mortality trade-offs, and observations leave little doubt that such difference exists.

4.7 Reliability

Variations in parameter values result in large variations in optimal depths, growth and mortality. The model is most sensitive to variations in parameters altering the M/F$_m$ ratio in the depth column, causing shifts in strategies (e.g. crepuscular and non-crepuscular feeding, adult migration), depth positions, growth and mortality. Surface light intensity is the dominant factor on optimal daytime depth, which was also observed in Masfjorden (GISKE, AKSNES, BALIÑO, KAARTVEDT, LIE, NORDEIDE, SALVANES, WAKILI and AADNESEN, 1990; BALIÑO and AKSNES, 1993). Stomach evacuation rate also influences the optimal depth position of juveniles, but to a lesser extent than surface light.

The model for visual feeding (AKSNES and GISKE, 1993) used to predict feeding rate and predation risk excludes important aspects in the foraging process. It does not account for movements of the prey which is important in both prey detection and attack success. It only accounts for horizontal vision and excludes the possible effects on prey detectability against

different background contrasts. All prey items are defined as spherical objects which excludes the effect of shape on visibility.

The fish are assumed to forage by vision only, and other mechanisms like the use of lateral-line organ (MONTGOMERY, 1989) and olfaction (ATEMA, HOLLAND and IKEHARA, 1980) are excluded from the foraging process. Only average values of prey size are represented at each depth, omitting the possibility of prey selection. However, in spite of these simplifications, the model matches the observations well.

The optimal feeding-mortality trade-offs predicted by the model depend heavily on the terminal fitness function defined, and the model is quite sensitive to variations in the steepness of the function. Using the terms of time and clutch manipulators suggested by AKSNES and GISKE (1990) relies on the assumption that the maximum adult size (maturity weight) is fixed, but plasticity in the relations between age, size and maturity is known to exist (STEARNS and CRANDALL, 1984). In a study of *M. muelleri* from eastern Australia, CLARK (1982) observed mature fish at 0.4g, and contrary to GJØSÆTER (1981) he found a significant positive correlation between fecundity and fish weight.

Seasonal variations in mortality-growth trade-offs is a problem if the relations between fitness, growth and mortality is to be established. Traditionally these relations are made throughout static expressions that do not account for possible time variations in trade-off rules. Using dynamic programming on annual scales where fitness could be linked directly to reproduction, this method could give the relations between growth, mortality and fitness at the time periods preceding the terminal time (i.e. reveal seasonal variations in the feeding-mortality trade-offs).

5. ACKNOWLEDGEMENTS

6. REFERENCES

AKSNES, D.L. and J. GISKE (1990) Habitat profitability in pelagic environment. *Marine Ecology Progress Series*, **64**, 209-215.

AKSNES, D.L. and J. GISKE (1993) A theoretical model of aquatic visual feeding. *Ecological Modelling*, **67**, 233-250.

ALEXANDER, R. McN. (1972) The energetics of vertical migration by fishes. *Symposium of the Society of Experimental Biology*, **26**, 273-294.

ATEMA, J., K. HOLLAND and W. IKEHARA (1980) Olfactory responses of yellowfin tuna (*Thunnus albaceres*) to prey odors: Chemical search image. *Journal of Chemical Ecology*, **6**, 457-465.

BALIÑO, B.M. and D.L. AKSNES (1993) Winter distribution and migration of the sound scattering layers, zooplankton and micronekton in the Masfjorden, western Norway. *Marine Ecology Progress Series*, **102**, 35-50.

BLAXTER, J.H.S. (1976) The role of light in the vertical migration of fish - a review. In: *Light as an ecological factor: II.* G.C. EVANS, R. BAINBRIDGE and OL RACKHAM, editors, Blackwell, London. 189-210.

BODEN, B. and E. KAMPA (1967) The influence of natural light on the vertical migrations of an animal community in the sea. *Symposium of the Zoological Society of London*, **19**, 15-26.

BOUSKILA, A. and T.D. BLUMSTEIN (1992) Rules of thumb for predation hazard assessment: Predictions from a dynamic model. *The American Naturalist*, **139**, 161-176.

BURROWS, M.T. and R.N. HUGHES (1991) Optimal foraging decisions by Dogwhelks, *Nucella lapillus* (L): Influences of mortality risk and rate constrained digestion. *Functional Ecology*, **5**, 461-475.

CARACO, T. (1980) On foraging time allocation in a stochastic environment. *Ecology*, **61**, 119-128.

CHILDRESS, J.J., S.M. TAYLOR, G.M. CAILLET and M.H. PRICE (1980) Patterns of growth, energy utilization and reproduction in some meso- and bathypelagic fishes off southern California. *Marine Biology*, **61**, 27-40.

CLARK, C.W. and D.A. LEVY (1988) Diel vertical distribution by juvenile sockeye salmon and the antipredation window. *The American Naturalist*, **131**, 271-288.

CLARK, C.W. and M. MANGEL (1986) The evolutionary advantages of group foraging. *Theoretical Population Biology*, **30**, 45-75.

CLARK, C.W. and R.C. YDENBERG (1990a) The risk of parenthood. I: General theory and applications. *Evolutionary Ecology*, **4**, 21-34.

CLARK, C.W. and R.C. YDENBERG (1990b) The risk of parenthood. II: Parent-offspring conflict. *Evolutionary Ecology*, **4**, 312-325.

CLARK, T.A. (1982) Distribution, growth and reproduction of the lightfish *Maurolicus muelleri* (Sternoptychidae) off South-East Australia. *CSIRO Marine Laboratory Report*, **145**, 10pp.

COLGAN, P. (1993) The motivational basis of fish behaviour. In: *Behaviour of teleost fishes*. T.J. PITCHER, editor, Chapman Hall, London, 31-55.

EGGERS, D.M. (1976) Theoretical effects of schooling by planktivorous fish predators on rate of prey consumption. *Journal of the Fisheries Research Board of Canada*, **33**, 1964-1971.

FALK-PETERSEN, I., S. FALK-PETERSEN and J.R. SARGENT (1986) Nature, origin and possible roles of lipid deposits in *Maurolicus muelleri* (Gmelin) and *Benthosema glaciale* (Reinhart) from Ullsfjorden, northern Norway. *Polar Biology*, **5**, 235-240.

FIKSEN, Ø. and J. GISKE (1993) *Documentation of a dynamic optimization model for the vertical distribution and population dynamics of a copepod cohort*. IFM Rapport 35/93. Department of Fisheries and Marine Biology, University of Bergen. 48 pp.

GELLER, W. (1986) Diurnal vertical migration of zooplankton in a temperate great lake (L. Constance): A starvation avoidance mechanism. *Archiev für Hydrobiologie Supplementband*, **74**, 1-60.

GEORGE, D.G. (1983) Interrelations between the vertical distribution of *Daphnia* and chlorophyll *a* in two large limnetic enclosures. *Journal of Plankton Research*, **5**, 457-475.

GILLIAM, J.F. (1982) *Habitat use and competitive bottlenecks in size-structured fish populations*. PhD Thesis, Michigan State University. 107pp.

GILLIAM, J.F. and D.F. FRASER (1987) Habitat selection under predation hazard: test of a model with foraging minnows. *Ecology*, **68**, 1856-1862.

GISKE, J. and D.L. AKSNES (1992) Ontogeny, season and trade-offs: vertical distribution of the mesopelagic fish *Maurolicus muelleri*. *Sarsia*, **77**, 253-261.

GISKE, J., D.L. AKSNES, B.M. BALIÑO, S. KAARTVEDT, U. LIE, J.T. NORDEIDE, A.G.V. SALVANES, S.M. WAKILI and A. AADNESEN (1990) Vertical distribution and trophic interactions of zooplankton and fish in Masfjorden, Norway. *Sarsia*, **75**, 65-81.

GISKE, J., D.L. AKSNES and Ø. FIKSEN (1994) Visual predators, environmental variables and zooplankton mortality risk. *Vie et Milieu*, **44**.

GISKE, J., D.L. AKSNES and B. FØRLAND (1993) Variable generation times and Darwinian fitness measures. *Evolutionary Ecology*, **7**, 233-239.

GJØSÆTER, J. (1981) Life history and ecology of *Maurolicus muelleri* (Gonostomatidae) in Norwegian waters. *Fiskeridirektoratets Skrifter Serie Havundersdkelser*, **17**, 109-131.

GJØSÆTER, J. (1986) Estimates of the abundance of mesopelagic fish off southern Norway and west of the British Isles 1971-1976. *Flødevigen rapportserie 1986* (1), 1-22.

HOLBROOK, S.J. and R.J. SCHMITT (1988) The combined effect of predation risk and food reward on patch selection. *Ecology*, **69**, 125-134.

HOLTBY, L.B. and M.C. HEALEY (1990) Sex-specific life history tactics and risk-taking in coho salmon. *Ecology*, **71**, 678-690.

HOUSTON, A., C. CLARK, J.M. MCNAMARA and M. MANGEL (1988) Dynamic models in behavioural and evolutionary ecology. *Nature*, **332**, 29-34.

HUNTLEY, M. and E.R. BROOKS (1982) Effects of age and food availability on diel vertical migration of *Calanus pacificus*. *Marine Biology*, **81**, 23-31.

IWASA, Y. (1982) Vertical migration of zooplankton: A game between predator and prey. *The American Naturalist*, **120**, 171-180.

JAKOBSEN, P.J., G.H. JOHNSEN and P. LARSSON (1988) Effects of predation risk and parasitism on the feeding ecology, habitat use, and abundance of lacustrine threespine sticklebacks (*Gasterosteus aculeatus*). *Canadian Journal of Fisheries and Aquatic Sciences*, **45**, 426-431.

JOBLING, M. (1981) Mathematical models of gastric emptying and the estimation of daily rates of food consumption for fish. *Journal of Fish Biology*, **19**, 245-257.

JOHNSEN, G.H. and P.J. JAKOBSEN (1987) The effect of food limitation on vertical migration in *Daphnia longispina*. *Limnology and Oceanography*, **32**, 873-880.

KAARTVEDT, S., D.L. AKSNES and A. AADNESEN (1988) Winter distribution of macroplankton and micronekton in Masfjorden, western Norway. *Marine Ecology Progress Series*, **45**, 45-55.

KATZ, P.L. (1974) A long-term approach to foraging optimization. *The American Naturalist*, **108**, 758-782.

KAWAGUCHI, K. and J. MAUCHLINE (1982) Biology of mycrophid fishes (family Myctophidae) in the Rockall Trough, northeastern Atlantic Ocean. *Biological Oceanography*, **1**, 337-373.

KAWAGUCHI, K. and J. MAUCHLINE (1987) Biology of sternoptychid fishes in the Rockall Trough, northeastern Atlantic Ocean. *Biological Oceanography*, **4**, 99-121.

KELLY, E.J. and P.L. KENNEDY (1993) A dynamic state variable model of mate desertion in cooper's hawks. *Ecology*, **74**, 351-366.

KIØRBOE, T., P. MUNK and K. RICHARDSON (1987) Respiration and growth of larval herring *Clupea harengus*: Relation between specific dynamic action and growth efficiency. *Marine Ecology Progress Series*, **40**, 1-10.

KIRK, J.O.T. (1981) Monte Carlo study of the nature of the underwater light field in, and the relationships between optical properties of, turbid yellow waters. *Australian Journal of Marine and Freshwater Research*, **32**, 517-532.

LEONARDSON, K. (1991) Predicting risk-taking behaviour from life-history theory using static optimization technique. *Oikos*, **60**, 149-154.

LEVY, D.A. (1990) Sensory mechanism and selective advantage for diel vertical migration in juvenile soceye salmon, *Oncorhynchus nerka*. *Canadian Journal of Fisheries and Aquatic Sciences*, **48**, 1796-1802.

LIE, U., T. MAGNESEN, B. TUNBERG and D.L. AKSNES (1983) Preliminary studies on the vertical distribution of size-fractions in the zooplankton community in Lindåspollene, western Norway. *Sarsia*, **68**, 65-80.

LOPEZ, P.D.C. (1979) Eggs and larvae of *Maurolicus muelleri* (Gonostomatidae) and other fish eggs and larvae from two fjords in western Norway. *Sarsia*, **64**, 199-210.

MAGNESEN, T., D.L. AKSNES and H.R. SKJOLDAL (1989) Fine-scale vertical structure of a summer zooplankton community in Lindåspollene, western Norway. *Sarsia*, **74**, 115-126.

MANGEL, M. and C.W. CLARK (1986) Towards a unified foraging theory. *Ecology*, **67**, 1127-1138.

MANGEL, M. and C.W. CLARK (1988) *Dynamic modelling in behavioural ecology*, Princeton University Press, Princeton, NJ. 308pp.

MASON, M.D. and E.W. PATRICK (1993) A model for the space-time dependence of feeding for pelagic fish populations. *Transactions of the American Fisheries Society*, **122**, 844-901.

MAUCHLINE, J. (1991) Some modern concepts in deep-sea pelagic studies: Patterns of growth in the different horizons. In: *Marine Biology. Its accomplishment and future prospects*. J. MAUCHLINE and T. NEMOTE, editors, Hokusen-sha, Tokyo, 107-130.

MCLAREN, I. (1963) Effects of temperature on growth of zooplankton and the adaptive value of vertical migration. *Journal of the Fisheries Research Board of Canada*, **20**, 685-727.

MCNAMARA, J.M. (1990) The policy which maximizes long-term survival of an animal faced with the risk of starvation and predation. *Advances in Applied Probability*, **22**, 295-308.

MCNAMARA, J.M. and A.I. HOUSTON (1992) State-dependent life-history theory and its implications for optimal clutch size. *Evolutionary Ecology*, **6**, 170-185.

MELO, Y.C. and M.J. ARMSTRONG (1991) Batch spawning behaviour in lightfish *Maurolicus muelleri*. *South African Journal of Marine Science*, **10**, 125-130.

METCALFE, N.B. and R.W. FURNESS (1984) Changing priorities: The effect of pre-migratory fatenning on the trade-off between foraging and vigilance. *Behavioural Ecology and Sociobiology*, **15**, 203-206.

MILINSKI, M. (1985) Risk of predation of parasitized sticklebacks (*Gasterosteus aculeatus* L.) under competition for food. *Behaviour*, **93**, 203-216.

MILINSKI, M. and R. HELLER (1978) Influence of a predator on the optimal foraging behaviour of sticklebacks, (*Gasterosteus aculeatus* L.). *Nature*, **275**, 642-644.

MONTGOMERY, J.C. (1989) Lateral line detection of planktonic prey. In: *Neurobiology of the mechanosensory lateral line*. S. COOMBS, P. GORNER and H. MUNTZ, editors, Springer-Verlag, New York, 561-574.

PRIEDE, I.G. (1985) Metabolic scope in fishes. In: *Fish energetics - new perspectives*. P. TYTLOW and P. CALOW, editors, Johns Hopkins, Baltimore, 33-64.

ROBERTSON, D.A. (1976) Planktonic stages of *Maurolicus muelleri* (Teleostei: Sternoptychidae) in New Zealand waters. *New Zealand Journal of Marine and Freshwater Research*, **10**, 311-328.

ROBINSON, C.J. and T.J. PITCHER (1989a) The influence of hunger and ration level on shoal density, polarization and swimming speed of herring, *Clupea harentus* L. *Journal of Fish Biology*, **34**, 631-633.

ROBINSON, C.J. and T.J. PITCHER (1989b) Hunger motivation as a promotor of different behaviours within a shoal of herring: Selection for homogeneity in fish shoal? *Journal of Fish Biology*, **35**, 459-460.

ROSENBERG, G.V. (1966) *Twilight - A study of atmospheric optics*. Plenum Press, New York. 358pp.

ROSLAND, R. (1993) *Documentation of a stochastic dynamic optimization model for the diel vertical distribution of a pelagic planktivore*. IFM Rapport 11/93. Department of Fisheries and Marine Biology, University of Bergen. 53pp.

SAMYSHEV, E.Z. and S.V. SCHETINKIN (1971) Feeding patterns of some species of Myctophidae and *Maurolicus muelleri* caught in the sound dispersing layers in the north-western African area. *Annales Biologique Conseil International pour l'Exploration de la Mer*, **28**, 212-215.

SARGENT, R.C. (1990) Behavioural and evolutionary ecology of fishes: Conflicting demands during the breeding season. *Annales Zoolici Fennici*, **27**, 101-118.

SCHAFFER, W.M. (1983) The application of optimal control theory to the general life-history problem. *The American Naturalist*, **121**, 418-431.

SCHMIDT-NIELSEN, K. (1983) *Animal physiology: Adaption and environment. 3rd edition*. Cambridge University Press, Cambridge, 619pp.

SKARTVEIT, A. and J.A. OLSETH (1988) *Varighetstabeller for timevis belysning mot 5 flater på 16 norske stasjoner*. Meteorological Report Series 7, Universitetet i Bergen. 136pp.

STEARNS, S.C. and R.E. CRANDALL (1984) Plasticity for age and size at sexual maturity: A life-history response to unavoidable stress. In: *Fish reproduction, strategies and tactics*. G.W. POTTS and R.J. WOOTTON, editors, Academic Press, London, 13-33.

STEPHENS, D.W. (1981) The logic of risk-sensitive foraging preferences. *Animal Behaviour*, **29**, 628-629.

STEPHENS, D.W. and E.L. CHARNOV (1982) Optimal foraging: Some simple stochastic models. *Behavioural Ecology and Sociobiology*, **10**, 251-263.

SUMIDA, B.H., A.I. HOUSTON, J.M. McNAMARA and W.D. HAMILTON (1990) Genetic algorithms and evolution. *Journal of Theoretical Biology*, **147**, 59-84.

WERNER, E.E. and J.F. GILLIAM (1984) The ontogenetic niche and species interactions in size-structured populations. *Annual Revue of Ecology and Systematics*, **15**, 393-425.

WERNER, E.E. and D.J. HALL (1988) Ontogenetic habitat shift in bluegill: The foraging rate-predation risk trade-off. *Ecology*, **69**, 1352-1356.

WERNER, E.E., J.F. GILLIAM, D.J. HALL and G.G. MITTELBACH (1983) An experimental test of the effects of predation risk on habitat use in fish. *Ecology*, **64**, 1540-1548.

WINDELL, J.T. (1978) Digestion and the daily ration of fishes. In: *Ecology of freshwater fish production*. S.D. GERKING, editor, Blackwell, London, 159-183.

WURTZBAUGH, W.A. and D. NEVERMAN (1988) Post-feeding thermotaxis and daily vertical migration in a larval fish. *Nature*, **333**, 846-848.

YDENBERG, R.C. (1989) Growth-mortality trade-offs and the evolution of the juvenile life histories in the Alcidae. *Ecology*, **70**, 1494-1506.

YOUNG, J.W. and S.J.M. BLABER (1986) Feeding ecology of three species of midwater fishes associated to the continental slope of eastern Tasmania, Australia. *Marine Biology*, **93**, 147-156.

YOUNG, J.W., S.J.M. BLABER and R. ROSE (1987) Reproductive biology of three species of midwater fishes associated with the continental slope of eastern Tasmania, Australia. *Marine Biology*, **95**, 323-332.